



Vulnerability assessment for climate adaptation planning in a Mediterranean basin

M. Alba Solans, Hector Macian-Sorribes, Francisco Martínez-Capel & Manuel Pulido-Velazquez

To cite this article: M. Alba Solans, Hector Macian-Sorribes, Francisco Martínez-Capel & Manuel Pulido-Velazquez (2024) Vulnerability assessment for climate adaptation planning in a Mediterranean basin, Hydrological Sciences Journal, 69:1, 21-45, DOI: [10.1080/02626667.2023.2219397](https://doi.org/10.1080/02626667.2023.2219397)

To link to this article: <https://doi.org/10.1080/02626667.2023.2219397>



© 2023 The Author(s). Published by Informa UK Limited, trading as Taylor & Francis Group.



Published online: 05 Dec 2023.



Submit your article to this journal [↗](#)



Article views: 633



View related articles [↗](#)



View Crossmark data [↗](#)

Vulnerability assessment for climate adaptation planning in a Mediterranean basin

M. Alba Solans ^a, Hector Macian-Sorribes ^a, Francisco Martínez-Capel ^b and Manuel Pulido-Velazquez ^a

^aResearch Institute of Water Engineering and Environment (IIAMA), Universitat Politècnica de València, València, Spain; ^bInstitut d'Investigació per a la Gestió Integrada de Zones Costaneres (IGIC), Universitat Politècnica de València, Gandia, Spain

ABSTRACT

The Iberian Peninsula is a climate change hotspot, where the temperature is increasing faster than the global annual mean surface temperature, with the largest reduction of precipitation. Consequently, freshwater availability is expected to decrease substantially. In this context, freshwater systems are especially vulnerable in terms of meeting the water demands and ecosystem requirements we know today. In this paper, we present an extension of the eco-engineering decision scaling (EEDS) method to explore trade-offs in agricultural and ecologic metrics at the catchment scale across a range of unknown future hydrological and climate states. The extended EEDS method evaluates current water resource management rules focusing on agricultural and ecologic objectives, identifies climate hazards that make the system fail and assesses climate risk in three time horizons for the design of adaptation measures. The case study is the Serpis River basin, Spain, where 72% of available water is used for agricultural purposes.

ARTICLE HISTORY

Received 29 June 2022
Accepted 17 March 2023

EDITOR

A. Castellarin

GUEST EDITOR

A. Sharma

KEYWORDS

decision scaling; integrated water resources management; climate stress testing; climate change adaptation; agricultural demands; environmental flows

1 Introduction



Climate action is at the heart of the European Green Deal (https://ec.europa.eu/info/strategy/priorities-2019-2024/european-green-deal_en), a series of political initiatives to lead the EU to climatic neutrality in 2050. Among its planned actions are the shift to a sustainable food system and the protection of biodiversity and ecosystems to make our environment more resilient to climate change.

There is a substantial scientific consensus that the Mediterranean region (MedR) is a climate change hotspot (Cramer *et al.* 2018). MedR is warming on average 20% faster than the global annual mean surface temperature (GMST) and, simultaneously, precipitation is decreasing by 4% for each degree of GMST increase (Lionello and Scarascia 2018). In the MedR context, the annual temperature increase is maximal over the Iberian Peninsula, especially in the summer, where locally the rate of change is twice that of GMST (Lionello and Scarascia 2018). The annual precipitation decrease with global warming is largest over Iberia, where the reduction is greater than 50 mm/°C (Lionello and Scarascia 2018). As a consequence, freshwater availability is likely to decrease substantially (by 2–15% for 2°C of warming) – among the most significant decreases in the world (Jiménez Cisneros *et al.* 2014, MedECC 2019, ACA 2020) – with significant increases in the length of meteorological dry spells (Kovats *et al.* 2014, Schleussner *et al.* 2016) and droughts (Tsanis *et al.* 2011). Along these lines, Hettiarachchi *et al.*

(2022) found a higher increment of the proportion of warm summers, defined from mean summer temperature, past the year 2000 in the USA, Europe, Asia and Australia. Within summer seasons, they found that the mean length of dry spells (0 mm of rain) was higher in warm summers with respect to colder summers in the same period, which means an increase in the stress on water availability in the last few years, and probably also in the years to come, as the climate is tending towards getting warmer.

Water use in the MedR is mainly for agriculture, accounting for more than 50% of total water use (Iglesias *et al.* 2011). When a region becomes drier and warmer, water crop demands increase because of an increase in crop evapotranspiration caused by increased temperatures (Döll 2002). MedR is a semi-arid region where reduction of water availability and increase in water crop demands may put agricultural activities and food security at risk (Iglesias *et al.* 2012, IPCC 2022).

Freshwater ecosystems are also particularly sensitive to warming since water quantity and quality are strongly influenced by atmospheric temperature regimes (Capon *et al.* 2021). On the one hand, air temperature determines water temperature and many chemical attributes contributing to water quality. Moreover, water temperature plays a key role in determining the distribution of freshwater species and influences most critical biological processes, including those associated with reproduction (e.g. spawning cues, triggers for egg hatching and seed germination, etc.), and growth (Visser *et al.* 2016). More specifically, the potential effects of warming on the habitat of salmonid fish species have been

CONTACT M. Alba Solans  malba.solans@gmail.com  Research Institute of Water Engineering and Environment (IIAMA), Universitat Politècnica de València, València, Spain

© 2023 The Author(s). Published by Informa UK Limited, trading as Taylor & Francis Group.

This is an Open Access article distributed under the terms of the Creative Commons Attribution-NonCommercial-NoDerivatives License (<http://creativecommons.org/licenses/by-nc-nd/4.0/>), which permits non-commercial re-use, distribution, and reproduction in any medium, provided the original work is properly cited, and is not altered, transformed, or built upon in any way. The terms on which this article has been published allow the posting of the Accepted Manuscript in a repository by the author(s) or with their consent.

analysed in some Mediterranean rivers (Almodóvar *et al.* 2012, Muñoz-Mas *et al.* 2016, 2018, Santiago *et al.* 2017). On the other hand, surface and groundwater regimes, including precipitation, snowmelt, runoff, soil moisture, river discharge, and aquifer recharge, are similarly sensitive to warming, with significant changes to hydrology to which native species will not necessarily have adapted (Cai and Cowan 2008, Capon *et al.* 2021). For example, He *et al.* (2022) found that in most regions, except for some tropical and sub-tropical regions, frequent flood volume (closely related to water supply storage) and flood peak are lower with higher temperatures, which is consistent with the recent historical declines in mean streamflow observed in southern Australia, southern Europe and large parts of the US (Gudmunsson *et al.* 2019).

Adaptive measures may be necessary to alleviate the negative impacts of climate change on socio-economic systems and freshwater ecosystems. Adaptability is part of resilience. It represents the capacity to adjust responses to changing external drivers and internal processes (Folke *et al.* 2010). Sustainable water systems, which meet the needs of society while maintaining key ecological functions, have more capacity to adapt and persist under changing social and environmental conditions (Poff *et al.* 2016).

Planning for resilient, robust and adaptive water systems to achieve social, economic and environmental objectives under non-stationary climate conditions is challenging (Poff *et al.* 2016). Traditionally, regional to local climate change impact assessments have used downscaled future climate projections from general circulation models (GCMs) to provide an ensemble of climate scenarios (Dessai and Hulme 2007, Brekke *et al.* 2009, Lempert and Groves 2010) and assess system vulnerabilities. However, the range of GCM results is a lower bound of the maximum range of future climate uncertainty (Stainforth *et al.* 2007). In addition, GCM predictions are difficult to interpret probabilistically (Tebaldi and Knutti 2007, Stephenson *et al.* 2012).

An alternative approach was presented by Brown *et al.* (2011) that described a decision-analytic based method called “decision scaling” (DS), aimed at creating climate response functions according to system vulnerabilities identified by a bottom-up process across a range of climate change conditions. Moreover, available top-down projections were informative of climatic conditions’ plausibility. Brown *et al.* (2012) introduced the term stakeholder-defined risk into the DS approach to identify system vulnerabilities based on what is important to stakeholders in terms of risk and impact. The DS approach is less sensitive to climate model uncertainties because it can identify system vulnerabilities potentially unrealized under downscaled GCM projections, and it can also utilize computationally efficient climate generation tools to better explore the effects of internal climate variability (Steinschneider *et al.* 2015b).

Poff *et al.* (2016) introduced the sustainable principle into the DS framework by adding the ecological dimension. The method, called “eco-engineering decision scaling” (EEDS), considers engineering and ecological performance to operationalize sustainable water resource management. In the EEDS approach, decision makers engage with stakeholders to determine ecological and engineering/economic metrics and critical thresholds of the system. In a multiple-objective DS approach, system vulnerability is

then assessed by evaluating the sensitivity of the metrics to a variety of non-stationary threats, such as climate change conditions. EEDS allows the evaluation of trade-offs between engineering-economic design and ecological performance, in complex social and ecological systems, to suggest management decisions.

Another significant contribution that evolved from DS is the climate risk informed decision analysis (CRIDA) approach of the United Nations Educational, Scientific and Cultural Organization (UNESCO) International Hydrological Programme. CRIDA is a bottom-up multi-step process to identify water security hazards and design robust adaptation pathways in line with the local needs, and with the participation, of local communities (UNESCO 2018). Like DS and EEDS, CRIDA aims at suggesting water resources management decisions while dealing with uncertain future climatic conditions.

This study presents a multi-objective decision framework applied in the Serpis River basin, a complex Mediterranean basin with three sub-basins that are interrelated climatically and hydrologically. We explore simultaneously the agricultural and environmental vulnerabilities of the basin due to the uncertain future climate forecasts. This work represents an extension of the EEDS that targets complex water systems, where climatic and streamflow variables from different sub-basins are spatially and temporally correlated and in which the operating rules and water allocation mechanisms are modelled in detail. The vulnerability assessment was carried out by applying a climatic stress test to the system, considering 20 climatic scenarios and forcing 434 simulations for each to explore possible potential climate fluctuations.

This study contributes to the goal of water resources planning in Spain, which is achieving water security for citizens and future generations and protecting biodiversity and socio-economic activities.

2 Study area

The Serpis River basin is located in a semi-arid region in eastern Spain and drains an area of 985 km² to the Mediterranean Sea. Within the Jucar River Basin District (managed by the Jucar Water Agency, hereafter CHJ), there are three main sub-basins, Beniarrés, Encantada and Vernissa, that are climatically and hydrologically interrelated (Fig. 1). The river is regulated by a single reservoir, Beniarrés (26.5 Hm³), whose main functions are irrigation supply and flood protection. Agricultural demands in the Serpis River basin account for 72% of the total water demands in the basin (CHJ 2022). The main agricultural demands are located in the lower basin and are Canales Altos (15.91 Hm³/year) and Canales Bajos (12.59 Hm³/year). While Canales Altos is supplied exclusively by surface water, Canales Bajos can use both surface and groundwater. Drinking water in the main urban areas of the basin is provided by groundwater.

Beniarrés dam was built in 1958, and since then the flow regime has been altered to some degree by the dam operation and several abstractions for irrigation downstream, with relevant impacts on the riparian communities. The Jucar River Basin Management Plan (JRBMP) (CHJ 2022) establishes minimum and maximum environmental flow regimes downstream of the dam as well as flood regimes and a rate of change at a daily and hourly time

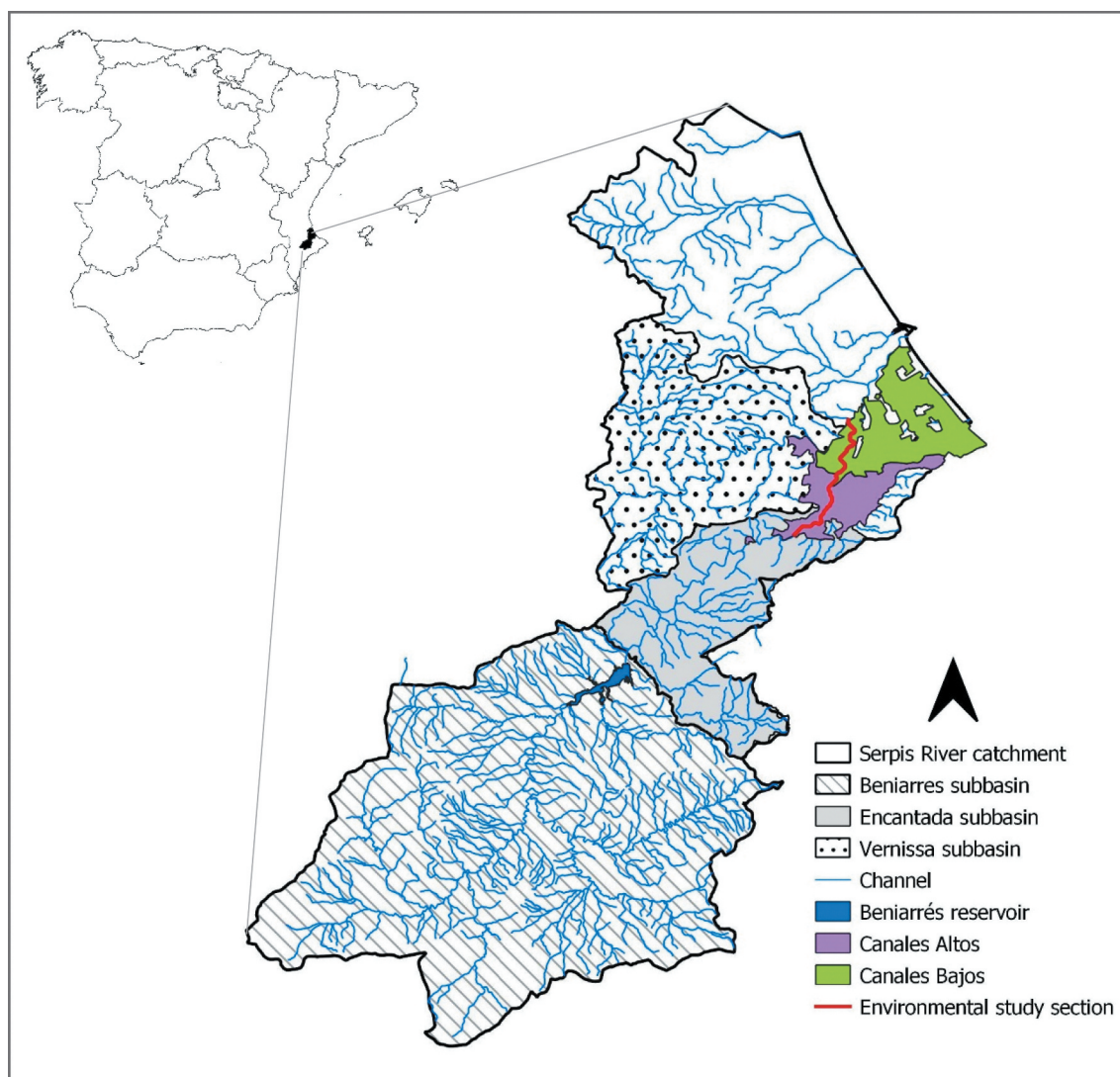


Figure 1. Case study: the Serpis River basin with three sub-basins, Beniarrés, Encantada and Vernissa. The agricultural demands (green and purple) and the river section (red) where environmental vulnerability is evaluated are highlighted.

scale. The present study focuses on the vulnerability of a specific section downstream of the Beniarrés dam concerning minimum and maximum environmental flows. It was selected because of its interest in terms of past experience and available information about aquatic habitats and species (Martínez Capel *et al.* 2018).

Climate data of precipitation (P) and temperature (T) for each sub-basin were obtained from Spain02_v5, a daily gridded set of observed data developed for the Iberian Peninsula and the Balearic Islands (Herrera *et al.* 2016). The data used in the present work comprises the period from January 1950 to December 2015. Observed climate data were spatially averaged at each sub-basin and were aggregated to the monthly time scale. Historical monthly inflows (Q) from Beniarrés, Encantada and Vernissa sub-basins were obtained from the CHJ webpage (www.chj.es) for the period 1971–2007.

3 Methodology

In the present work, we disclose a decision system framework to assess the climatic vulnerability of a Mediterranean basin

under climate change conditions, focusing on agricultural demands and ecological requirements.

First, a weather generator corresponding to each sub-basin was developed to generate multiple realizations of climate variability (P and T), and we performed a climatic stress test on the basin at the monthly time scale. The weather generator consists first of an autoregressive model (AR) at the annual scale, followed by a subsequent disaggregation at the monthly scale, and finally the elaboration of climate change scenarios through the alteration of some time series statistics.

Subsequently, a hydrological model previously calibrated transformed climatic data into streamflow data. A water resource system model estimated the system's response to the hydrological uncertainty and developed and identified the critical conditions that made the system fail according to some previously defined economic (agricultural) and ecologic metrics. The plausibility of the climatic conditions was cross-checked by comparing them with the climate patterns derived from an ensemble of 22 GCM projections from five scenarios from the Coupled Model Intercomparison Project Phase 6

(CMIP6), combining Shared Socioeconomic Pathways (SSP) and Representative Concentration Pathways (RCP) scenarios for the period between 2011 and 2099 (Table 1). These projections were bias-adjusted on the mean statistic following the methodology applied by the Spanish Meteorology Agency (Amblar *et al.* 2017) and the Sixth Assessment Report of the Intergovernmental Panel on Climate Change (IPCC 2021). Figure 2 shows the different steps of the model, which are described below.

3.1 Weather generator

We developed a weather generator based on the works of Steinschneider and Brown (2013) and Steinschneider *et al.* (2015a).

First, we used AR models to generate synthetic annual precipitation and temperature time series at each sub-basin to catch climatic low-frequency signals. The synthetic series had the same length as the historical series (65 years) and

Table 1. Ensemble of the Global Climate Model (GCM) projections considered in the study for the different Coupled Model Intercomparison Project Phase 6 (CMIP6) scenarios evaluated for precipitation (P) and temperature (T) shaded cells mean unavailable or unused GCM - scenario combinations.

GCM/Scenario	SSP1_1.9	SSP1_2.6	SSP2_4.5	SSP3_7.0	SSP5_8.5
CANESM (Can)					
ACCESS-CM(Aus)					
BCC-CSM2-CM (Chi)					
CESM2 (USA)					
CMCC-CM2-SR5 (Ita)					
CMCC-ESM2 (Ita)					
CNRM-CM6 (Fra)					
CNRM-ESM2(Fra)					
FGOALS_G3 (Chi)					
GFDL-ESM4 (USA)					
HADGEM-GC31-11 (UK)					
IITM-ESM (Ind)					
INM-CM4.8 (Rus)					
INM-CM5.0 (Rus)					
IPSL-CM6A-LR (Fra)					
KACE-1.0-G (Kor)					
MIROC6 (Jap)					
MIROC-ES2L (Jap)					
MPI-ESM1-2-LR (Ger)					
MRI-ESM2 (Jap)					
NORES2-MM (Nor)					
UKESM1.0_LL (UK)					

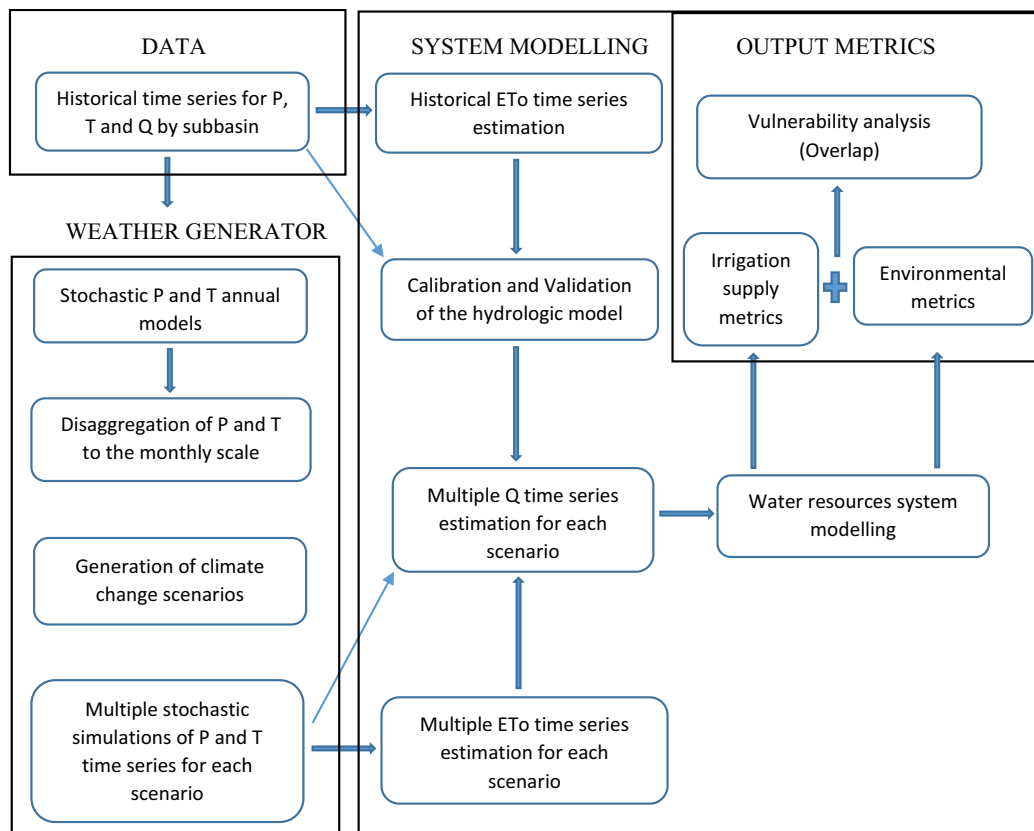


Figure 2. Flowchart of the vulnerability assessment framework.

closely preserved historical main statistics (mean, standard deviation, correlation structure and cross-correlation across sub-basins).

For precipitation, the historical annual time series fulfilled the normality and stationarity requirements of AR models; thus, no transformation was applied. After appropriate analyses, we found that the most suitable model was an AR(0) model (i.e. no autocorrelation):

$$X_t = \mu + \sigma * \varepsilon_t \quad (1)$$

where μ is the time series mean, σ is the standard deviation, and ε_t is the residual noise term, which is independent and distributed according to a white noise process. Additionally, because of the high correlation between the data of the different sites, we added a linear correlation structure to the models:

$$\text{Encantada} : \varepsilon_t^{(\text{Encantada})} = 0.9223 * \varepsilon_t^{(\text{Beniarrés})} + \eta_t \quad (2)$$

$$\begin{aligned} \text{Vernisa} : \varepsilon_t^{(\text{Vernisa})} \\ = -0.365 * \varepsilon_t^{(\text{Beniarrés})} + 1.315 * \varepsilon_t^{(\text{Encantada})} + \eta_t \end{aligned} \quad (3)$$

where η_t are independent normal random variables with mean zero, and the regression parameters were obtained from historical time series relationships.

Annual time series were disaggregated to the monthly time step using the method of fragments (Srikanthan and McMahon 2001). It consisted, first, of calculating the proportion of annual P corresponding to each month in each year of the historical series, obtaining a range of fragments. Afterwards, the order of the range was randomly altered for each simulation, and the new range of factors was applied to the synthetic time series. This method maintains the intra-annual correlation of the variable.

Finally, we generated several alternative climate change scenarios by altering the mean statistic of the series in order to explore the basin performance outside the historical uncertainty. The changes in the mean consisted of applying variations from -30% to $+30\%$, using increments of 15% (five increments), in accordance with precipitation projections observed in the GCM projections taken into account in the study. The new 65-year precipitation time series were obtained by quantile mapping, representing the period 2015–2080.

Regarding temperature (T), high cross-correlation between the historical monthly time series at the different sub-basins was found ($R^2 > 0.99$). Therefore, we decided to build a weather generator for temperature in the Encantada sub-basin at annual scale in order to catch climatic low-frequency signals, and subsequently estimate the corresponding time series for the other sub-basins, through linear regression models at the monthly scale. The annual model for the Encantada sub-basin was developed after removing the tendency of the historical annual series and confirming the normality of the stationary series. The analyses indicated that the most appropriate model to estimate the synthetic T time series was an AR(2) model (i.e. a lag-2 autocorrelation model):

$$Y_t = \mu + \Phi_1 * z_{t-1} + \Phi_2 * z_{t-2} + \sigma_\varepsilon * \xi_t \quad (4)$$

where μ is the time series mean; σ_ε is the standard deviation of the residual term; z_{t-1} and z_{t-2} are $y_{t-1} - \mu$ and $y_{t-2} - \mu$,

Table 2. Climate changes included in the stress test.

Type of change	Minimum	Maximum	Number of scenarios
Mean precipitation	-30%	$+30\%$	5
Mean temperature	0	$+3^\circ\text{C}$	4

respectively; ξ_t is the residual noise term, which is independent and distributed according to a white noise process; and Φ_1 and Φ_2 are the AR model coefficients.

Climate change scenarios for T were formulated at the annual scale by forcing increments in the mean from 0 to 3°C through the period (2015–2080), by increments of 1°C (four increments). The maximum increment interval was defined based on the maximum change in global surface temperature in the short- and mid-term periods (2021–2060) (IPCC 2021). A standard additive method was used to alter the temperature distribution. The annual adding factor increased gradually for the entire simulation period, starting at 0 and ending at the level of a specified change (e.g. 2°C).

Monthly time series for Encantada were obtained after disaggregating annual time series by using the method of fragments (Srikanthan and McMahon 2001). Subsequently, monthly, area-averaged temperature time series for Beniarrés and Vernisa sub-basins were obtained through the linear regressions shown below:

$$T^{(\text{Beniarrés})} = 1.0008 * T^{(\text{Encantada})} - 1.4575 \quad (5)$$

$$T^{(\text{Vernisa})} = 0.9945 * T^{(\text{Encantada})} + 0.8121 \quad (6)$$

where the regression parameters and the error terms were obtained from historical time series relationships. At the end of the weather generator modelling process, 20 (5×4) climate change scenarios were considered (Table 2).

3.2 Estimation of evapotranspiration time series

Reference evapotranspiration (ET_o) time series were estimated from monthly temperature time series after applying a transformation factor (TF). Consequently, the stochastic model generates alternative T time series that are then transformed into ET_o time series. The TF was specific for each sub-basin, and it was obtained at representative climatic stations that fulfilled three conditions: (1) they provide historical mean monthly temperature (T_{CS}) data and Penman-Monteith (PM) reference evapotranspiration (ET_o) data; (2) T_{CS} and ET_o time series are highly correlated; and (3) temperature time series from climatic stations (T_{CS}) are highly correlated with the corresponding series from Spain02_v5 dataset (T) (see Table 3).

TFs were quantified as the ratio between monthly ET_o and monthly T_{CS} time series at each climatic station. To apply the TF to the new generated temperature time series, we estimated the mean periodic ratio by Fourier series representation (Salas et al. 1997). We assumed that the relationship between ET_o and T would remain stationary despite changes in climate conditions.

Table 3. Historical temperature (T_{CS}) and reference evapotranspiration (ETo) data series at each climatic station used for ETo estimation. R-squared (R^2) coefficients refer to T_{CS} and basin averaged historical temperature (T) series from Spain02_v5.

Sub-basin	Climatic station	R^2 between T time series ⁽²⁾	T_{CS} and ETo data series ⁽¹⁾
Beniarrés	Planes	0.98	December 1999 – December 2015
Encantada	Vilallonga	0.98	April 2001 – December 2015
Vernisa	Gandía Marxuquera	0.99	April 2001 – December 2015

3.3 Hydrological and water resources system modelling

We used the Témez rainfall–runoff model (Témez 1977) to transform each climatic simulation into a streamflow time series. The Témez model is a conceptual lumped hydrological model that considers the sub-basin as a homogeneous unit. To calibrate and validate the model, we used the historical monthly averaged areal precipitation (P) and reference evapotranspiration (ETo) time series for each sub-basin as input variables, and historical streamflow time series (Q) at each sub-basin as output variables. An optimization tool that minimized the root mean square error (RMSE) carried out the calibration of the parameters and we used four goodness-of-fit indices to evaluate the model's accuracy: RMSE, Nash-Sutcliffe efficiency coefficient (E), R^2 and integral square error (ISE).

Once the calibration of the rainfall–runoff model was completed, we transformed the climatic simulations generated by the weather generators into streamflow time series, which were used as inputs for a water resources system model representing the Serpis River basin (Fig. 3). The system model was built with the GAMS software (Brooke *et al.* 1998) to estimate the system's performance under each simulated climate change condition. This system includes the precipitation inputs of the three main sub-basins, reaches and canals of the Serpis River, the Beniarrés reservoir, two urban demands (UDUs) and two agricultural (D1 and D2)

demands, and the two principal aquifers of the Serpis River basin. The characteristics of the components were obtained from the JRBMP.

The acceptable performance of the Serpis River basin was defined in terms of a trade-off between satisfying the two objectives defined in the system: agricultural water supply reliability and environmental flow requirements. The level of satisfaction of each objective was measured according to some thresholds that indicated whether the performance of the metric was optimum, acceptable or not acceptable. The metrics used in the assessment are described below.

3.3.1 Agricultural metrics

The main agricultural demands supplied by the Serpis River correspond to two irrigation districts: Canales Altos (D1, 15.91 Hm³/year) and Canales Bajos (D2, 12.59 Hm³/year), both located in the lower Serpis (see Fig. 1). The metric used to represent the agro-economic objective of the system is the proportion of annual demand met each year. The acceptance threshold of the variable was set at 50%, as is established in the Spanish water law. Moreover, we considered that water supply below the current average level, approximately 75% in both demands, was not satisfactory for farmers due to the economic impact. Therefore, a second threshold was set at 75% of the water volume demanded for one year to indicate an optimum supply.

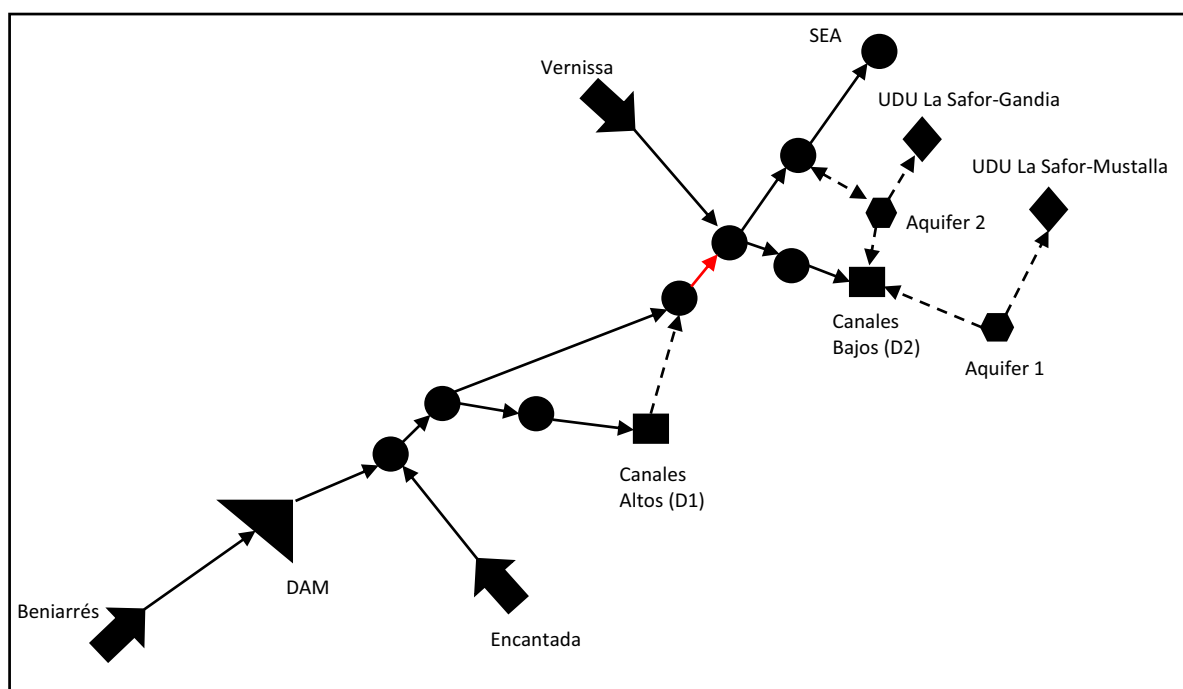


Figure 3. Water resources system model of the Serpis River basin.

Table 4. Minimum and maximum environmental flow regimes (m^3/s) in the study section, according to the JRBMP, and $Q_{\text{transition}}$ considered for Q_{max} tolerance.

	October	November	December	January	February	March	April	May	June	July	August	September
Q_{min}	0.25	0.25	0.28	0.32	0.32	0.40	0.35	0.28	0.25	0.25	0.25	0.25
Q_{max}	1.4	6.4	6.4	6.4	6.4	1.4	1.4	1.4	1.4	1.4	1.4	1.4
$Q_{\text{transition}}$	1.75	8	8	8	8	1.75	1.75	1.75	1.75	1.75	1.75	1.75

Table 5. Criteria to evaluate the performance of the Serpis River basin according to agricultural (economic) and environmental objectives.

		Ecological objective		
		Q monthly mean $> Q_{\text{transition}}$	$Q_{\text{transition}} > Q$ monthly mean $> Q_{\text{max}}$	Q monthly mean $< Q_{\text{max}}$
Agricultural (economic) objective	Mean annual supply in D1 or D2 $< 50\%$	NOT ACCEPTED	NOT ACCEPTED	NOT ACCEPTED
	$50\% >$ mean annual supply in D1 and D2 $< 75\%$	NOT ACCEPTED	ACCEPTED	ACCEPTED
	Mean annual supply in D1 and D2 $> 75\%$	NOT ACCEPTED	ACCEPTED	OPTIMUM

3.3.2 Environmental metrics

The JRBMP establishes an environmental flow regime in the rivers across the basin with the aim to sustain the ecological function of some aquatic protected species and their habitats. The environmental flow regime in the JRBMP consists of (a) a minimum flow regime (Q_{min}) extended to all superficial water bodies at a monthly scale, and (b) a maximum flow regime (Q_{max}) at a monthly scale in regulated water bodies. In the present work, we evaluated the implementation of minimum (Q_{min}) and maximum (Q_{max}) environmental flow regimes in a specific river reach below the dam (see section 2: Study area). The thresholds of acceptable performance for each variable were extracted from the JRBMP (see Table 4). Q_{min} thresholds were considered a restriction in the water management model, since the JRBMP holds that minimum flows are compulsory for ecological requirements. With respect to Q_{max} , JRBMP marks different periods: a wet season (from November to February) and a dry season (from March to October). In addition, we assumed that a monthly streamflow of up to 25% over Q_{max} could be considered acceptable

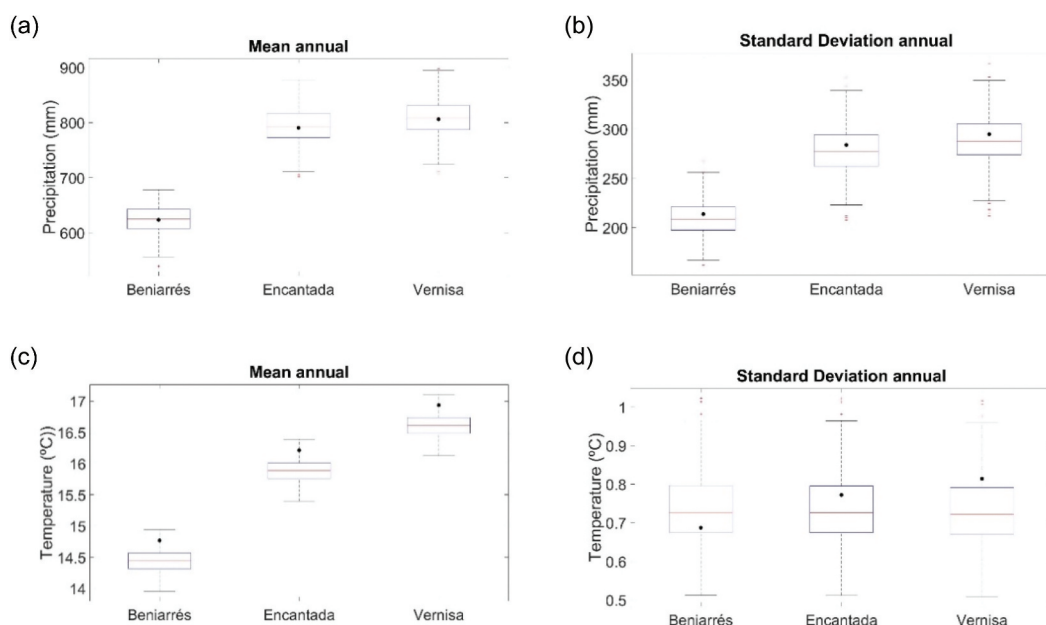
for practical reasons in the analyses. This “tolerance” or extended threshold for Q_{max} was called $Q_{\text{transition}}$.

To evaluate the robustness of the basin performance and explore model uncertainty, we generated 434 P and T runs for each climate scenario using MATLAB® (Steinschneider *et al.* 2015a, Poff *et al.* 2016, John *et al.* 2021). After estimating the ET_0 for each run and obtaining the corresponding hydrological scenario from the Témez model, we evaluated whether the climatic scenario provided an acceptable or not acceptable performance of the system according to the trade-off between the objectives’ metrics results (Table 5). A plan is considered robust if it can provide satisfying performance for a weighted proportion of simulations.

4 Results

4.1 Weather generator

Figure 4 displays the box-whisker plots of the annual mean and standard deviation obtained for the 434 65-year-long


Figure 4. Mean and standard deviation of the 434 synthetic simulations over the 65-year annual time series for precipitation (a, b) and temperature time series (c, d) at Beniarrés sub-basin.

synthetic time series of P and T. The results indicate that for precipitation the median values for both statistics fit the historical values (black dots) in all sub-basins. In contrast, for temperatures the median values show some bias, especially the mean, which is underestimated by 0.3 to 0.4°C.

Once the simulations were downscaled at the monthly scale, the same statistics were verified. Figure 5 shows the results for Beniarrés statistics as an example, while Appendix Figs A1 and A2 present the results for the other two sub-basins.

We obtained satisfactory precipitation results, especially in the Beniarrés sub-basin (Fig. 5(a) and (b)). The maximum bias in the mean monthly precipitation in Encantada and Vernissa sub-basins was about 20 mm in November, which is the wettest month.

For temperature (Fig. 5(c) and (d)), the mean monthly estimations were slightly underestimated with respect to historical values for all sub-basins, which is in line with the annual-scale tendency. However, the maximum bias was about 0.5–0.6°C, corresponding to the hottest month, August.

4.2 Estimation of evapotranspiration time series

Figure 6 shows the ETo time series estimated in the Beniarrés sub-basin (red dashed line) and the historical time series from the correspondent climatic station (black fill line). It allows us to observe the goodness of fit of minima, maxima and periodicity. Encantada and Vernissa ETo estimations are given in Appendix Fig. A3, and they show a similar performance.

Table 6 shows some of the characteristics of the TFs obtained at each sub-basin by the Fourier series model (number of harmonics and percentage of variance explained) and some goodness-of-fit statistics of the ETo estimated time series. For example, we can observe that only one or two harmonics were needed to catch almost the total variability of the mean monthly historical TF time series. The estimated ETo time series explained about 96–98% of ETo observations in the three sub-basins, and RMSE was around 10 mm/month in all of them. Therefore, we considered that the transformed factors obtained were appropriate to estimate ETo data from synthetic T time series.

4.3 Hydrological and water resource system modelling

The available streamflow data was split into two time periods to calibrate (1971–2000) and validate (2001–2007) the rainfall–runoff model. Table 7 shows calibration and validation results obtained for the three sub-basins. For calibration, the R^2 ranged between 0.69 and 0.88, and E was between 0.69 and 0.86, which indicates a good reproduction of the historical behaviour. RMSE and ISE also show adequate performance levels, in line with R^2 and E. Validation results show, in general, a slight decrease of the performance level, as expected, with the exceptions of the E index for Encantada (from 0.86 to 0.40) and all indices except ISE from Beniarrés (which shows an increase in performance). Since the drop observed in the E index for Encantada is not reflected in the rest of the metrics, it can be concluded that the hydrological Témex models offer

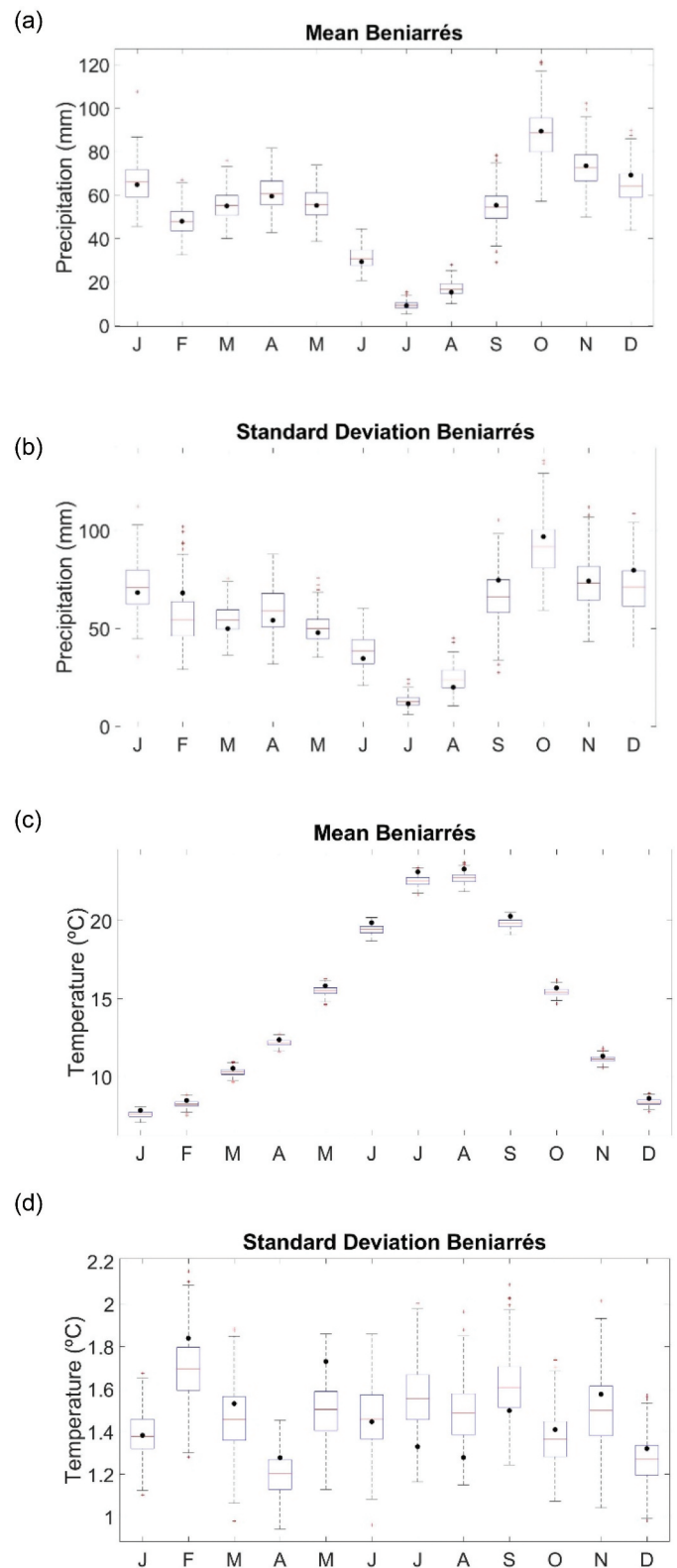


Figure 5. Mean and standard deviation of the 434 synthetic simulations over the 65-year monthly precipitation (a, b) and temperature (c, d) time series at Beniarrés sub-basin.

a fair reproduction of the historical hydrological behaviour of the Serpis basin.

Figure 7 shows the observed (black fill line) and the simulated (red dashed line) discharges in the Beniarrés sub-basin (see

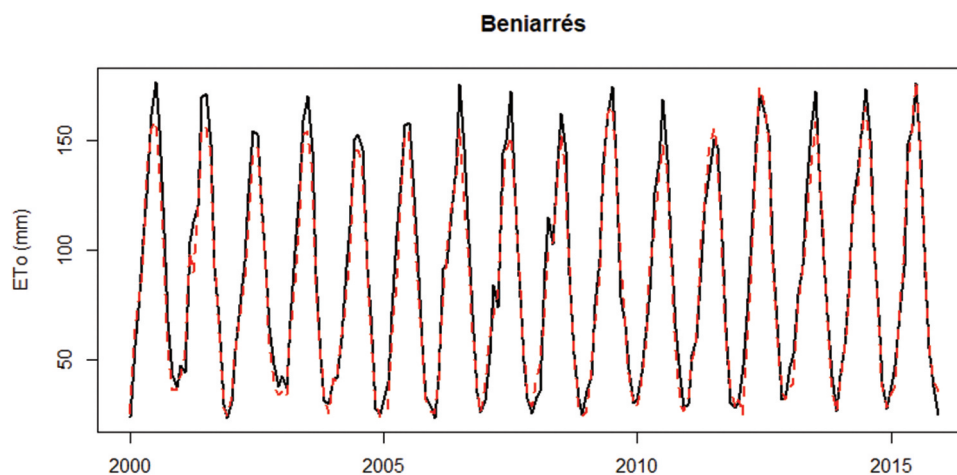


Figure 6. Historical (black) and estimated (dashed red) ETo monthly time series in Beniarrés sub-basin.

Table 6. Characteristics of the periodic transformation factor (TF) used in each sub-basin (Beniarrés, Encantada and Vernissa) to estimate ETo, as well as some goodness-of-fit statistics for monthly ETo time series estimations (R^2 and RMSE).

Sub-basin	No. harmonics (h) of TF	Variability explained by h (% over the total variance of periodic mean estimate)	R^2 between historical and simulated ETo data	RMSE between historical and simulated ETo data (mm/month)
Beniarrés	2	99.76	0.98	8.43
Encantada	2	99.75	0.96	10.12
Vernissa	1	99.17	0.97	7.68

Table 7. Goodness-of-fit statistics: RMSE, Nash-Sutcliffe efficiency coefficient (E), R^2 and integral square error (ISE) of the Téméz model in calibration and validation processes in the three sub-basins: Beniarrés, Encantada and Vernissa.

Sub-basin	Calibration (1971–2000)				Validation (2001–2007)			
	RMSE	E	R^2	ISE	RMSE	E	R^2	ISE
Beniarrés	2.79	0.69	0.69	0.62	1.89	0.81	0.84	0.62
Encantada	0.64	0.86	0.88	0.69	1.43	0.40	0.72	0.82
Vernisa	0.90	0.71	0.75	1.06	1.40	0.64	0.69	1.12

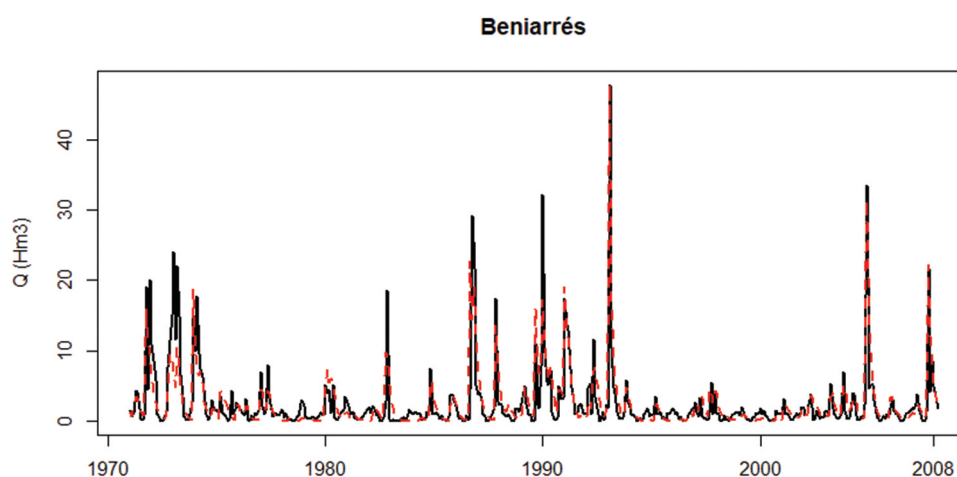


Figure 7. Historical (black) and estimated (dashed red) hydrograph in Beniarrés sub-basin.

graphs for the other sub-basins in Appendix Fig. A4). The plots show that the models capture precisely the low and high stream-flow frequency in the three sub-basins along the whole series, with some underestimation in the high-flow pulses.

After the calibration and validation process, 434 runs of 65-year-long synthetic time series of P and ETo (the latter obtained from the simulated T time series), with the 20 climate change

scenarios associated with each run, were transformed into the corresponding hydrological discharges. These discharges were used as inputs into the water resource system model to determine the main variables associated with water resource management (releases and storage from Beniarrés reservoir, streamflow, deliveries and deficits), from which the agricultural and environmental metrics were quantified.

4.4 Performance measures and robustness

The performance of the system for each hydrological run was evaluated independently at all the objective metrics, which were classified as *optimum*, *acceptable* or *not acceptable*, according to the thresholds described above.

When focusing on agricultural metrics (Fig. 8), we observed that optimum performance (green) occurred in both demands (D1 and D2) when mean monthly precipitation was equal to or above the historical records. However, the acceptable performance, $\geq 50\%$ annual demand satisfied, orange class, failed in D1 for precipitation reductions higher than 25% with respect to historical records, while D2 could cope with reductions of up to 30% because of its possibility to use groundwater. Therefore, we found that the D1 supply was more vulnerable than the D2.

An important issue to highlight is that the variation in mean annual temperature across scenarios did not seem to alter the annual water supply performance. This occurred because, in the present research work, we kept the agricultural water

demands uniform across all climatic scenarios in line with water rights specified in the JRBMP (CHJ 2022). Future increments in water rights (demands) are subject to the existence of sufficient water resources and the approval of the JRBMP. Therefore, given the uncertainty about the evolution of water rights in the future, we considered the current water rights a proper proxy for future water demands.

Concerning the environmental metrics, the minimum environmental flows (Q_{min}) were satisfied under all scenarios evaluated, since they were prescribed for the model as is established in the JRBMP and the dam operating rules. Consequently, the only environmental metric evaluated in the following was the maximum monthly environmental flow (Q_{max}), in which we observed noticeable differences throughout the year (Fig. 9). During the wet period (from November to February), we observed that in most climatic conditions, the mean monthly flow in the study river section was satisfactory concerning both the Q_{max} defined in JRBMP (green) and the $Q_{transition}$ (tolerance zone) defined in the present work (orange).

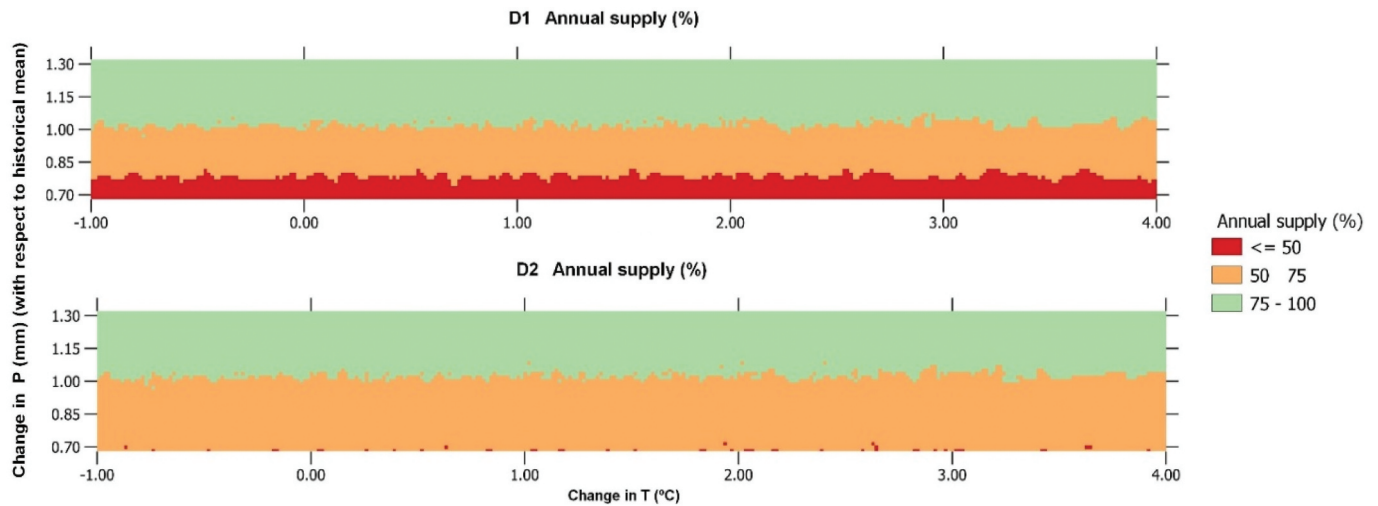


Figure 8. Representation of the gradient of annual supply (%) in D1 (Canales Altos) and D2 (Canales Bajos) across all the evaluated climatic conditions.

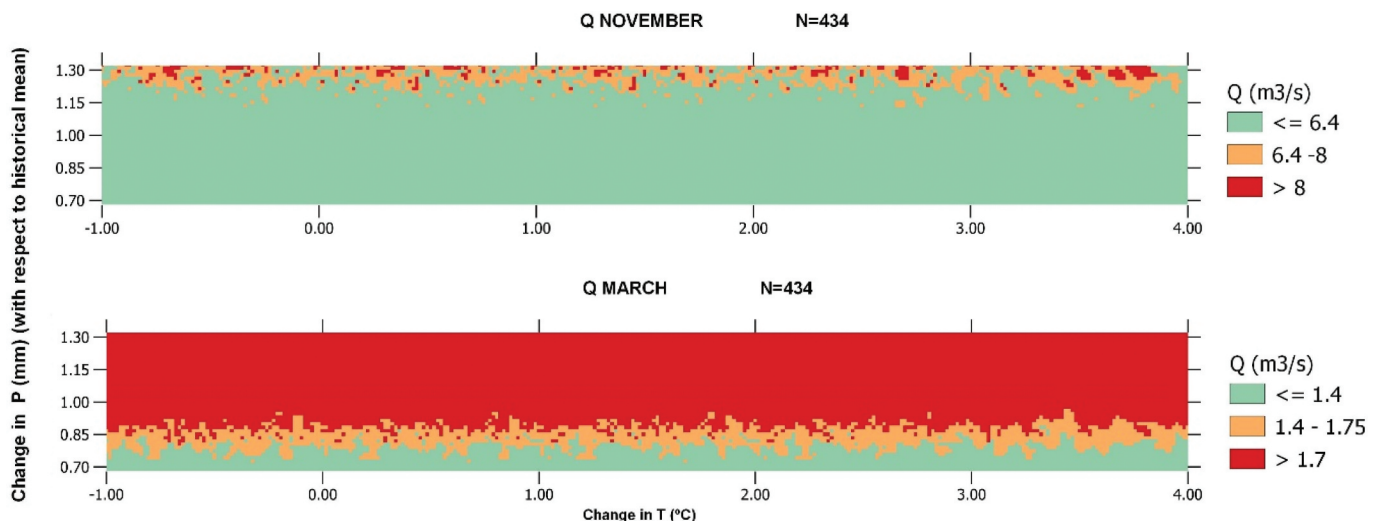


Figure 9. Representation of the gradient of mean monthly flow in the study section in November (wet period) and March (dry period) across all the evaluated climatic conditions.

Conversely, during the dry period (from March to October), the mean monthly flow surpassed the Q_{max} and $Q_{transition}$ thresholds frequently (red zone), unless the precipitation dropped significantly from historical records (about 15–20% or even 25% depending on the month). Important to highlight is the fact that even under the present climatic conditions the maximum environmental flow threshold set in the

JRBMP is not met during this period, probably because of the current Beniarrés operating rules.

When agricultural and environmental metrics were overlapped to find a common domain, we obtained a space that permitted us to evaluate the concurrent degree of satisfaction of the system objectives across climate change conditions. Figures 10 and 11 show some examples of the trade-

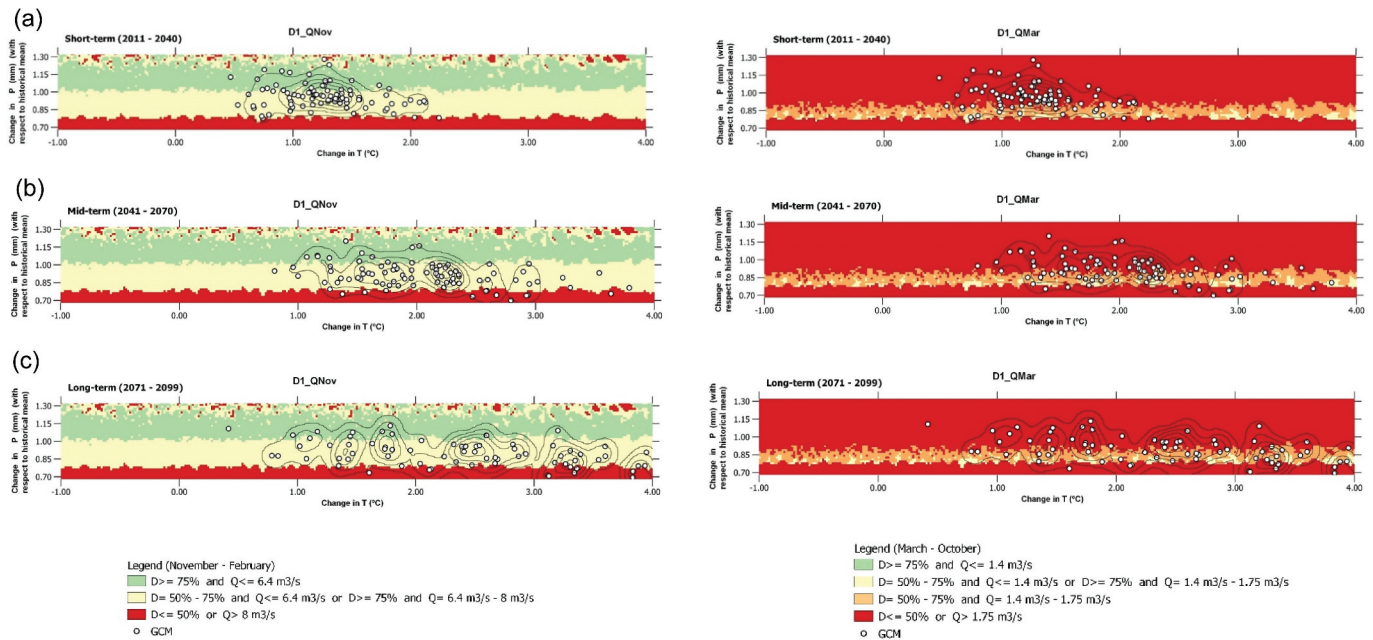


Figure 10. Overlapping maps of mutually acceptable performance (trade-off space) for the two indicators (agricultural demand supply and environmental maximum flow) for agricultural demand D1 and the mean monthly flow in the study river reach across a range of climatic conditions. In the left column, as an example, are the maps for November (wet period) and in the right column are the maps for March (dry period). The white dots represent an ensemble of GCM projections from CMIP6 in three temporal periods: (a) short term, (b) mid term, and (c) long term.

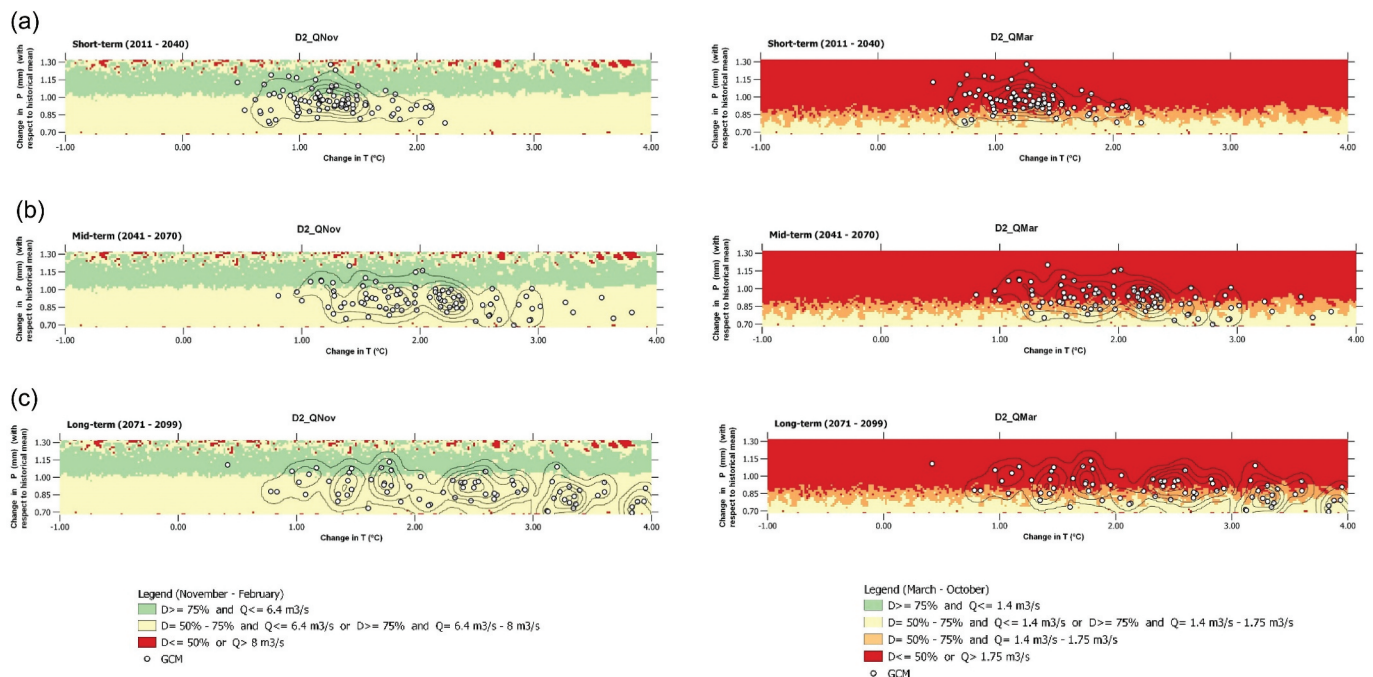


Figure 11. Overlapping maps of mutually acceptable performance (trade-off space) for the two indicators (agricultural demand supply and environmental maximum flow) for agricultural demand D2 and the mean monthly flow in the study river reach across a range of climatic conditions. In the left column, as an example, are the maps for November (wet period) and in the right column are the maps for March (dry period). The white dots represent an ensemble of GCM projections from CMIP6 in three temporal periods: (a) short term, (b) mid term, and (c) long term.

off space obtained in Canales Altos (D1) and in Canales Bajos (D2) demands, respectively, in the wet and dry periods. The results for the rest of the year are shown in the Appendix (Figs A5–A10). We can observe that the trade-off space consists of an acceptable zone divided into three sub-zones according to the degree of suitability (Table 5): green zone when both variables are optimum, yellow zone when one of the variables is optimum and the other is acceptable, and orange zone when both variables are acceptable. The red zone indicates unacceptable performance. We can see evident differences in the acceptable area in the wet versus the dry period in both demands. During the wet period (November–February), the acceptable zone in both demands occupies almost all the climatic space evaluated. However, during the dry period (March–October), nearly all the scenarios failed to satisfy the system objectives since the acceptable zone appears only with significant reductions in precipitation. The discrepancies in results between wet and dry seasons are mainly due to the significant difference in the Q_{max} threshold for both periods. During the dry period, when the Q_{max} threshold is relatively low, the mean monthly streamflow easily exceeds it with current management rules and, therefore, the performance becomes unacceptable. This issue was observed even under the present climatic conditions, which indicates that the system's performance during the dry period is conditioned by factors other than climate change. In particular, the current system operation seems to be the origin of the system failure during the dry period, and, thus, its adaptation is required to meet the environmental flow prescriptions of JRBM and ensure the sustainability of the water system. Another evident difference between D1 and D2 results was the major vulnerability of D1 because of its complete dependency on superficial streamflow, already mentioned in the agricultural metrics results.

An ensemble of GCM projections from CMIP6 (Table 1) helped in figuring out the feasibility of future climate scenarios in three temporal scenarios: short term (2011–2040), mid term (2041–2070) and long term (2071–2099). When analysing the results for each period, we estimated climate plausibility based on the convergence of GCMs and then identified potential impacts in the system associated with climate conditions.

For example, in Figs 10(a) and 11(a), we observe that in the short term, GCM predictions match in a relatively small climate space, which is perceived as having a high probability of occurrence. The majority of the models are located around a small range of precipitation change (85–110%) with an increment of mean annual temperature between 1 and 1.5°C. In these conditions, according to our results, the yearly supply to meet agricultural demands would be similar to the current levels (around 70–75%). Therefore, in the short term, no adaptive measures, or very limited ones, should be needed in the basin.

In the mid term (2041–2070), GCM projections show a wider spread, which means higher uncertainty among climatic model forecasts (see Figs 10(b) and 11(b)). Two main clusters of projection models can be identified that foresee a higher probability of precipitation reductions of up to 25% with respect to historical records. Although these climatic projections are inside the acceptable zone, they would cause

an increase in demand deficits (annual supply between 50 and 75%). Therefore, adaptive measures in the mid term should be considered to balance the water scarcity and the consequent economic impact on the agro-economic system. Moreover, D1 would be especially vulnerable since precipitation reductions of ca. 25% would drop it near the limit of acceptance.

Although our climate test represented the conditions for short and mid time periods, especially for temperature, we also evaluated climate plausibility in the long term (2071–2099). We observed a significant uncertainty in GCM projections across emission scenarios in the long term (see Figs 10(c) and 11(c)). The models with the most optimistic scenarios (SSP1-1.9 and SSP1-2.6, representative of the Paris Agreement) indicate future climatic conditions not far from those described in the short- and mid-term scenarios. Nevertheless, many models with the most pessimistic emission scenarios (SSP3-7.0 and SSP5-8.5) foresee reductions in precipitation of up to 30% and a mean annual temperature rise of more than 3°C, consistent with the expected temperature rise (IPPC 2021). Adaptive strategies in the long term are difficult to anticipate because of the high uncertainty in current climate forecasts. Nevertheless, if any are undertaken, they should be flexible in responding to the extensive range of socio-economic scenarios and climatic conditions we will potentially face.

5 Discussion

We present an alternative method to the traditional top-down GCM framework to make impact assessments in water-dependent economies while addressing climate uncertainty. The method we present here permits us to evaluate a high range of climate change conditions through a computationally efficient climate generation tool, and explore basin robustness against climate variability. Assessing the vulnerability of the system is fundamental to anticipating potential risks and designing suitable adaptable strategies or pathways to overcome climate change hazards and achieve resiliency. The methodology presented in this paper is an extension of the DS (Brown *et al.* 2012) and EEDS (Poff *et al.* 2016) methods, which are bottom-up frameworks for achieving the principles of sustainability and stakeholder governance in the water planning process. We tested the framework in a complex Mediterranean basin, the Serpis River basin, with three climatically and hydrologically interrelated sub-basins, to evaluate agricultural supply reliability and freshwater habitat sustainability risks under uncertain climate conditions.

We identified that a significant precipitation reduction is likely to challenge the system in the mid and long term. Such a reduction in water resources would imply a substantial decrease in the agricultural water supply. Given that more than 70% of the total water demand in the Serpis River basin comes from agriculture, a considerable decrease in water supply would greatly impact the region's economy. For example, we identified that a reduction of 25% in annual precipitation would be critical for the Canales Altos demand (D1) since the system would fail to supply the minimum water required, and this scenario would be aligned with the mid-term projections of the CMIP6 GCMs. Therefore, this work exposes the need to

apply adaptive measures in the mid term, especially for D1 demand, to balance the expected water availability loss.

The present work also identified that current operating rules in Beniarrés dam do not consider the maximum environmental flows prescribed in JRBMP during the dry season. Aquatic species and habitats are adapted to the natural flow regime (Poff *et al.* 1997), and many biological processes are synchronized with the varying flow conditions. Any alteration in these conditions may lead to the impairment of freshwater ecosystems and even the extinction of some species (e.g. the brown Muñoz-Mas *et al.* 2016, 2018). Therefore, a review of present rules should be considered to encompass agricultural uses and environmental protection, while taking into account the further reductions in water resources expected in the future according to future climate projections (IPCC 2021).

The weather generator developed in the present work obtained satisfactory results in the validation process, reproducing spatial and temporal dynamics and correlation structures of the variables of interest. On the annual scale, precipitation statistics showed high robustness in the three sub-basins, and a slight bias in annual temperatures. The same trend was observed on the monthly scale. Moreover, the models could reproduce the monthly intra-annual variability of both P and T, which is essential for hydrological applications. The weather generator developed in the present work assumes no change in intra-annual patterns for future climate scenarios with respect to historical pattern, as well as a stationary cross-correlation between sub-basins. According to Hettiarachchi *et al.* (2022), dry spells' length should increase after 2000 during the summer season, which could imply changes in the precipitation seasonal cycle. However, comparing the precipitation pattern of two time periods in the basin corresponding to the Beniarrés sub-basin – 1950–1999 versus 2000–2015 – no significant differences were observed at the monthly scale (see Fig. 12). Therefore, we assumed that the increment of the length of dry spells at a daily time scale, if it occurred in the basin, did not impact on annual and monthly

patterns. A reason for this could be the irregular pattern of precipitation events in the Mediterranean region that could soften any small change on a daily scale. Shifts in intra-annual patterns, if found or desired to be taken into account in future scenarios, could be addressed in the proposed methodology by modifying the method of fragments to enable shifts in the seasonal cycle, or by applying an additional stochastic model to generate monthly time series from the annual ones. Further research would be required to explore alternative configurations of the downscaling from the annual to the monthly time scale in situations implying changes in the intra-annual meteorological cycle.

In the same way, we did not observe changes in cross-correlation between basins either (see Table 8), so we used the same models built from historical data to generate future climate change scenarios. However, a previous analysis of changes in climatic inter-relationships in the basin is fundamental to assume stationarity of model parameters and spatial structure. Likewise, any other potential change in streamflow pattern due to warming, like changes in snowmelt patterns, should be previously evaluated and incorporated in the formulation of the model when the catchment in focus requires it.

In the present research, we contributed a new method to efficiently obtain PM reference evapotranspiration (ET_o) time series from temperature (T) time series. It is generally considered that ET_o estimation is more accurate when using the PM method (Allen *et al.* 2006). However, the PM method requires a large number of variables, which are only available for some climatic stations in Spain (e.g. solar radiation, air humidity, wind velocity). Therefore, estimation of ET_o time series with the PM method is usually a tedious process (Camargo *et al.* 1999, Estrela *et al.* 1999, Pereira and Pruitt 2004). In the present work we provide a new method to agilely convert T time series into ET_o time series through the Fourier series model with high accuracy ($R^2 > 0.96$). This method is replicable in other regions when there are enough historical climatic data to compute the TFs with confidence.

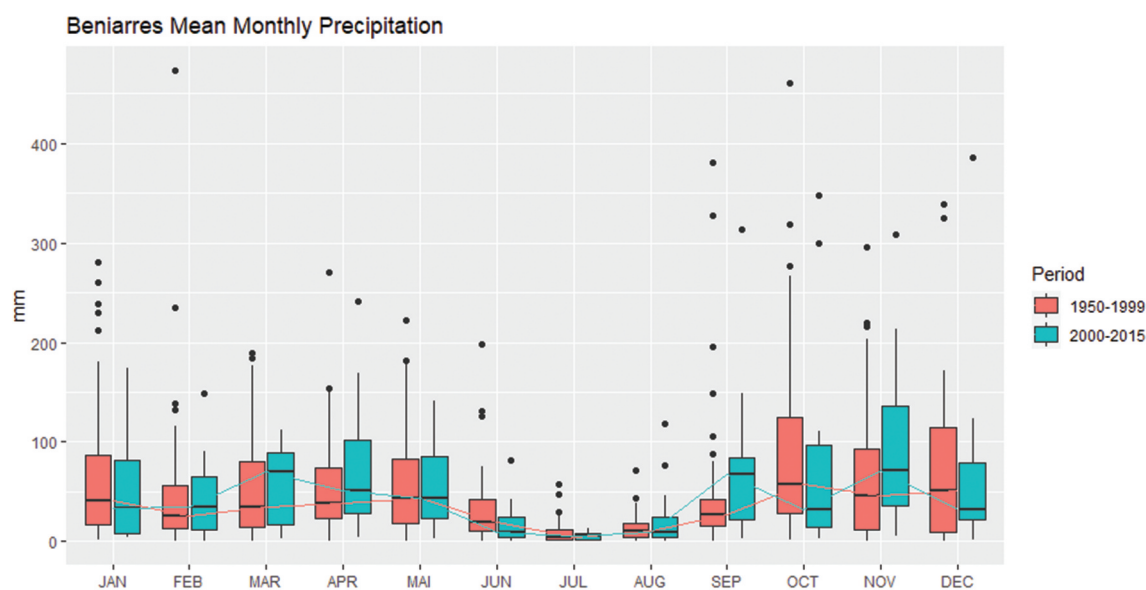


Figure 12. Mean monthly precipitation pattern in Beniarrés sub-basin in two time periods: 1950–1999 (red) and 2000–2015 (green).

Table 8. Cross-correlation between historical precipitation time series for Beniarrés (BRR), Encantada (ENC) and Vernisa (VER) sub-basins in two periods: 1950–1999 and 2000–2015.

	1950–1999	2000–2015
Correlation BRR-ENC	0.920	0.941
Correlation BRR-VER	0.847	0.868
Correlation ENC-VER	0.978	0.980

The present work aims at testing a methodological tool to give an idea of catchment water challenges under uncertain climate change conditions. The use of metrics at the monthly (monthly streamflow) or yearly (% annual water supply) scale permits us to give a first impression of potential hazards in the basin and contextualize planning actions. Nevertheless, recent findings give evidence that warming affects the water cycle and the relationship between extreme precipitation events and floods, which occur at daily or sub-daily level, especially from 2000 (Dai 2012, Sharma *et al.* 2018, He *et al.* 2022, Hettiarachchi *et al.* 2022). This phenomenon would alter rainfall–runoff models and, therefore, we evaluated any change in precipitation–streamflow relationship during historical data. We obtained the correlation between mean monthly precipitation and mean monthly streamflow in two time periods, 1971–1999 and 2000–2015, to identify any loss in correlation in the post-2000 period with respect to the pre-2000 period (see Table 9).

We observe that in the Encantada and Vernisa sub-basins the relationship is higher than 0.8 in both periods with no significant difference between the before- and after-2000 periods. In Beniarrés sub-basin the correlation is in fact stronger in the after-2000 period. Therefore, we confirmed that any loss in the correlation between precipitation and streamflow after 2000, if it occurred, was not reflected at the monthly scale, and consequently, we could use the same hydrological models in the two periods. Many reasons could explain the stationarity of the precipitation–streamflow relationship found in the Serpis River basin, e.g. the level of aggregation of the data, the size of the basin, the pattern of precipitation, or the scarce data available post-2000 period. We advocate evaluating this relationship before applying the present methodology in a different catchment.

The use of a monthly time step was chosen for the analysis because it is in line with the water planning focus of the application. This might imply that changes in daily and sub-daily extremes are not addressed properly. However, the practical implications of such changes in the water planning and management of the case study area are very low, since the storage capacity of the reservoir does not allow it to take advantage of such events to refill, and furthermore the areas prone to these events are located near the coastline, downstream of any regulation facility, so in the end changes in these

Table 9. Correlation between historical precipitation and streamflow time series in two periods, 1971–1999 and 2000–2015, in Beniarrés, Encantada and Vernisa sub-basins.

	1971–1999	2000–2015
Beniarrés	0.637	0.779
Encantada	0.868	0.808
Vernisa	0.829	0.821

events would only have a distinct impact in the discharges to the sea. However, the methodology proposed could be tuned to address such issues by adding an additional downscaling method from the monthly to the daily scale, or by replacing the downscaling from annual to the monthly scale by another one that maps the annual directly to the daily scale.

Regarding the future temperature scenarios, we forced a maximum rise of 3°C at the end of the period with respect to current records. However, due to stochastic effects in model generation the real rise was up to 4°C in many simulations. Therefore, it encompassed the best temperature estimation of IPCC6 for the period 2021 to 2100 (IPCC 2021). The temperature models applied in the present work assumed a constant rising trend along the future time period. Nevertheless, the methodology could accommodate alternative setups of temperature increase with varying trends, e.g. following the same trend for part of the time series and an increased trend for the rest. This would be achieved by modifying the model used for the generation of annual temperatures.

According to the EEDS methodology, the next step after analysing the vulnerability of the system would be the evaluation of the system performance after applying management actions and/or adaptive measures that stakeholders would have previously defined. The identification of preferred decisions was discussed in a previous project funded by the Biodiversity Foundation of the Ministry for the Ecological Transition of Spain (<https://www.fundacion-biodiversidad.es/en/node/10906> and <https://www.fundacion-biodiversidad.es/en/node/11884>), as well as in collaboration with the Citizen Platform for the Serpis River (<https://plataformaserpis.wordpress.com/>). In those projects, workshops and questionnaires were developed with the primary users, stakeholders and decision makers of the Serpis. According to their points of view, the most preferred options to deal with climate change were the use of treated wastewater (scored 7.8 over 10), closely followed by improving the operation of the Serpis (7.6) and improving the governance of the river as a whole (7.4). They also indicated that they would agree to assume an economic loss associated with a streamflow reduction of 25% maximum resulting from the climate change effects, which is in line with the agricultural thresholds marked in the present study. The proposed methodology would be able to accommodate those measures by modifying the definition of the water resource system.

However, the present study also highlighted some aspects of the methodology with room for improvement. The low influence that temperature exerts on the water resource system across climate change scenarios is due to the consideration of water demands under the legal point, which might not be aligned with the demand crop water requirements. This issue could be addressed by incorporating crop models into the water resource system to estimate agricultural water needs according to warming temperatures. Another aspect of the system that would be interesting to explore is the impact of warming on streamflow habitats, which should be addressed by the incorporation of ecological models (Horne *et al.* 2018, John *et al.* 2021).

The present work simultaneously deals with the vulnerability of socio-economic and environmental objectives in

the Serpis River basin to define sustainable water resource management in the face of future hydrological uncertainty. This work addresses, on the one hand, the evaluation of the current multi-purpose water management system and, on the other hand, the identification of potential climate hazards that would not satisfy the system objectives in the future. Vulnerability assessment is crucial for water planners to anticipate the climate risk of the system and take action towards building a resilient management framework.

6 Conclusions

Stress testing methods are an effective way to assess the sensitivity of water system outcomes to uncertain changes in climate. The methodology followed in the present work, an extension of the EEDS method to complex water resource systems, was successfully applied to the Serpis River basin. Herein, the stochastic weather generators, the ETo estimation by Fourier series model, hydrological models and water resource system models showed adequate performance levels compared to the existing records. In addition, the modelling framework has the capacity to be adapted to other systems with different characteristics and needs. The methodology applied has proven to robustly identify potential climate hazards to the system in different temporal horizons. It permitted us to identify the limitation of the system to supply Canales Altos (D1) demand in the mid term, which is crucial to anticipate adaptive strategies and minimize climate change impacts.

The methodology also revealed shortcomings in the present system management rules; in particular, it does not consider the maximum environmental flow regime downstream of the Beniarrés dam during the dry period. It would require, therefore, a modification of the Beniarrés dam operation to meet the legal ecological targets.

Sustainable water planning is a challenge for decision makers due to the huge number of stakeholders involved. Water systems management is a complex puzzle where any imbalance in water users produces inverse consequences for the others. Good water governance is essential to achieve water security, fairly allocate water resources, and avoid disputes. How societies choose to govern their water resources and services has a profound impact on people's livelihoods and the sustainability of water resources. Moreover, anticipating climate change impacts on water availability is the best way to avoid its adverse effects on societies and become resilient to changes.

Acknowledgements

The authors thank the two reviewers of the manuscript, Dr Ashish Sharma and an anonymous reviewer, for making substantial improvements.

Disclosure statement

No potential conflict of interest was reported by the authors.

Funding

This study was supported by the ADAPTAMED project [RTI2018-101483-B-I00], funded by the Ministerio de Economía y Competitividad (MINECO) of Spain and with EU FEDER funds. This research also received support from the SOS-WATER project [Grant Agreement No. 101059264] under the European Union's Horizon EUROPE Research and Innovation Programme.

ORCID

M. Alba Solans  <http://orcid.org/0000-0002-3508-270X>
 Hector Macian-Sorribes  <http://orcid.org/0000-0003-4077-9955>
 Francisco Martínez-Capel  <http://orcid.org/0000-0003-4991-0251>
 Manuel Pulido-Velazquez  <http://orcid.org/0000-0001-7009-6130>

References

- ACA, 2020. Documento IMPRESS 2019. Memoria. Estudio general de la demarcación, análisis de impactos y presiones de la actividad humana, y análisis económico del uso del agua en las masas de agua en el distrito de cuenca fluvial de Cataluña. Agència Catalana de l'Aigua. Departament de Territori i Sostenibilitat de la Generalitat de Catalunya. Available from: http://aca.gencat.cat/web/.content/30_Plans_i_programes/10_Pla_de_gestio/document_IMPRESS/IMPRESS-2019-memoria_es.pdf.
- Allen, R., *et al.*, 2006. Evapotranspiration del cultivo. Guías para la determinación de los requerimientos de agua de los cultivos. Estudio FAO Riego Y Drenaje No 56.
- Almodóvar, A., *et al.*, 2012. Global warming threatens the persistence of Mediterranean brown trout. *Global Change Biology*, 18 (5), 1549–1560. doi:10.1111/j.1365-2486.2011.02608.x.
- Amblar, P., *et al.*, 2017. *Guía de escenarios regionalizados de cambio climático sobre España a partir de los resultados de cambio climático sobre España*. Madrid: Ministerio de Agricultura y Pesca, Alimentación y Medio Ambiente, Agencia Estatal de Meteorología.
- Brekke, L.D., *et al.*, 2009. Assessing reservoir operations risk under climate change. *Water Resources Research*, 45, W04411. doi:10.1029/2008WR006941
- Brooke, A., *et al.*, 1998. *GAMS: a user's guide*. Washington: GAMS Development Corporation.
- Brown, C., *et al.*, 2012. Decision scaling: linking bottom-up vulnerability analysis with climate projections in the water sector. *Water Resources Research*, 48, W09537. doi:10.1029/2011WR011212
- Brown, C., *et al.*, 2011. A decision-analytic approach to managing climate risks: application to the upper great lakes. *Journal of the American Water Resources Association*, 47 (3), 524–534. doi:10.1111/j.1752-1688.2011.00552.x.
- Cai, W. and Cowan, T., 2008. Evidence of impacts from rising temperature on inflows to the Murray-Darling basin. *Geophysical Research Letters*, 35, LO7701. doi:10.1029/2008gl033390
- Camargo, A.P., *et al.*, 1999. Adjust of the Thornthwaite's method to estimate the potential evapotranspiration for arid and superhumid climates, based on daily temperature amplitude. *Revista Brasileira de Agrometeorologia*, 7 (2), 251–257.
- Capon, S.J., Stewart-Koster, B., and S.e, B., 2021. Future of freshwater ecosystems in a 1.5°C warmer world. *Frontiers in Environmental Science*, 9, 784642. doi:10.3389/fenvs.2021.784642
- Confederación Hidrográfica del Júcar, 2022. Plan Hidrológico de la Demarcación Hidrográfica del Júcar. Available from: <https://www.chj.es/es-es/medioambiente/planificacionhidrologica/Paginas/PHC-2021-2027-Indice.aspx>
- Cramer, W., *et al.*, 2018. Climate change and interconnected risks to sustainable development in the Mediterranean. *Nature Climate Change*, 8 (11), 972–980. doi:10.1038/s41558-018-0299-2-hal-01911390.
- Dai, A., 2012. Increasing drought under global warming in observations and models. *Nature Climate Change*, 3 (1), 52–58. doi:10.1038/nclimate1633.

- Dessai, S. and Hulme, M., 2007. Assessing the robustness of adaptation decisions to climate change uncertainties: a case study on water resources management in the East of England. *Global Environmental Change*, 17 (1), 59–72. doi:10.1016/j.gloenvcha.2006.11.005.
- Döll, P., 2002. Impact of climate change and variability on irrigation requirements: a global perspective. *Climatic Change*, 54, 269–293. doi:10.1023/A:1016124032231
- Estrela, T., Cabezas, F., and Estrada, F., 1999. La evaluación de los recursos hídricos en el Libro Blanco del Agua en España. *Ingeniería del agua*, 6 (2), 1886–4996. doi:10.4995/ia.1999.2781.
- Folke, C., et al., 2010. Resilience thinking: integrating resilience, adaptability and transformability. *Ecology and Society*, 15 (4), 20. Available from: <http://www.ecologyandsociety.org/vol15/iss4/art20/>
- Gudmunsson, I., et al., 2019. Observed trends in global indicators of mean and extreme streamflow. *Geophysical Research Letters*, 46, 756–766. doi:10.1029/2018GL079725
- He, W., et al., 2022. A global assessment of change in flood volume with surface air temperature. *Advances in Water Resources*, 165 (104241), 104241. doi:10.1016/j.advwatres.2022.104241.
- Herrera, S., Fernández, J., and Gutiérrez, J.M., 2016. Update of the Spain02 gridded observational dataset for Euro-CORDEX evaluation: assessing the effect of the interpolation methodology. *International Journal of Climatology*, 36 (2), 900–908. doi:10.1002/joc.4391.
- Hettiarachchi, S., Wasko, C., and Sharma, A., 2022. Do longer dry spells associated with warmer years compound the stress on global water resources? *Earth's Future*, 10 (e2021EF002392). doi:10.1029/2021EF002392.
- Horne, A.C., et al., 2018. Informing environmental water management decisions: using conditional probability networks to address the information needs of planning and implementation cycles. *Environmental Management*, 61, 347–357. doi:10.1007/s00267-017-0874-8
- Iglesias, A., et al., 2011. Towards adaptation of agriculture to climate change in the Mediterranean. *Regional Environmental Change*, 11, 159–166. doi:10.1007/s10113-010-0187-4
- Iglesias, A., et al., 2012. From climate change impacts to the development of adaptation strategies: challenges for agriculture in Europe. *Climatic Change*, 112 (1), 143–168. doi:10.1007/s10584-011-0344-x.
- IPCC, 2021. Summary for Policymakers. In: V. Masson-Delmotte, et al., eds. *Climate change 2021: the physical science basis. Contribution of working group I to the sixth assessment report of the intergovernmental panel on climate change*. Cambridge, UK and New York, NY: Cambridge University Press, 3–32. doi:10.1017/9781009157896.001.
- IPCC, 2022. *Climate change 2022: impacts, adaptation and vulnerability. Contribution of working group II to the sixth assessment report of the Intergovernmental Panel on climate change*. Cambridge, UK and New York, NY: Cambridge University Press, 3056. doi:10.1017/9781009325844
- Jiménez Cisneros, B.E., et al., 2014. Impacts, adaptation, and vulnerability. In, and C.B. Field, et al., eds. *Climate change*. New York, NY: IPCC, Cambridge Univ. Press, Ch. 3.
- John, A., et al., 2021. Robust climate change adaptation for environmental flows in the Goulburn River, Australia. *Frontiers in Environmental Science*, 9, 789206. doi:10.3389/fenvs.2021.789206
- Kovats, R.S., et al., 2014. Impacts, adaptation, and vulnerability. In, and C. B. Field, et al., eds. *Climate change*. New York, NY: IPCC, Cambridge Univ. Press, Ch. 23.
- Lempert, R.J. and Groves, D.G., 2010. Identifying and evaluating robust adaptive policy responses to climate change for water management agencies in the American West. *Technological Forecasting and Social Change*, 77, 960–974. doi:10.1016/j.techfore.2010.04.007
- Lionello, P. and Scarascia, L., 2018. The relation between climate change in the Mediterranean region and global warming. *Regional Environmental Change*, 18 (5), 1481–1493. doi:10.1007/s10113-018-1290-1.
- Martínez Capel, F., et al., 2018. *Adaptación al cambio global: gestión integral del régimen ecológico de carduales para el hábitat de la anguila europea y el cacho valenciano frente a especies invasoras. Informe detallado - 2018*. Gandia: Universitat Politècnica de València.
- MedECC, 2019. Risks associated to climate and environmental changes in the Mediterranean region. A preliminary assessment by the MedECC network science-policy interface – 2019. Mediterranean Experts on Climate and Environmental Change (MedECC) supported by the Union for the Mediterranean and Plan Bleu (UNEP/MAP Regional Activity Center). Available from: http://www.medecc.org/wp-content/uploads/2018/12/MedECC-Booklet_EN_WEB.pdf.
- Muñoz-Mas, R., et al., 2016. Shifts in the suitable habitat available for brown trout (*Salmo trutta* L.) under short-term climate change scenarios. *Science of the Total Environment*, 544, 686–700. doi:10.1016/j.scitotenv.2015.11.147
- Muñoz-Mas, R., et al., 2018. Combining literature-based and data-driven fuzzy models to predict brown trout (*Salmo trutta* L.) spawning habitat degradation induced by climate change. *Ecological Modelling*, 386, 98–114. doi:10.1016/j.ecolmodel.2018.08.012
- Pereira, A.R. and Pruitt, W.O., 2004. Adaptation of the Thornthwaite scheme for estimating daily reference evapotranspiration. *Agricultural Water Management*, 66 (3), 251–257. doi:10.1016/j.agwat.2003.11.003.
- Poff, N.L., et al., 1997. The natural flow regime. *BioScience*, 47 (11), 769–784. doi:10.2307/1313099.
- Poff, N.L., et al., 2016. Sustainable water management under future uncertainty with eco-engineering decision scaling. *Nature Climate Change*, 6 (1), 25–34. doi:10.1038/nclimate2765.
- Salas, J.D., et al., 1997. *Applied modelling of hydrologic time series*. 4th ed. Colorado: Water Resources Publications.
- Santiago, J.M., et al., 2017. Waning habitats due to climate change: the effects of changes in streamflow and temperature at the rear edge of the distribution of a cold-water fish. *Hydrology and Earth System Sciences*, 21 (8), 4073–4101. doi:10.5194/hess-21-4073-2017.
- Schleussner, C.F., et al., 2016. Differential climate impacts for policy-relevant limits to global warming: the case of 1.5 C and 2 C. *Earth System Dynamics*, 7 (2), 327–351. doi:10.5194/esd-7-327-2016.
- Sharma, A., Wasko, C., and Lettenmaier, D.P., 2018. If precipitation extremes are increasing, why aren't floods? *Water Resources Research*, 54, 8545–8551. doi:10.1029/2018WR023749
- Srikanthan, R. and McMahon, T.A., 2001. Stochastic generation of annual, monthly and daily climate data: a review. *Hydrology and Earth System Sciences*, 5 (4), 653–670. doi:10.5194/hess-5-653-2001.
- Stainforth, D.A., et al., 2007. Issues in the interpretation of climate model ensembles to inform decisions. *Philosophical Transactions of the Royal Society A: Mathematical, Physical and Engineering Sciences*, 365 (1857), 2163–2177. doi:10.1098/rsta.2007.2073.
- Steinschneider, S., et al., 2015a. Expanded decision-scaling framework to select robust long-term water-system plans under hydroclimatic uncertainties. *Journal of Water Resources Planning and Management*, 141 (11), 04015023. doi:10.1061/(ASCE)WR.1943-5452.0000536.
- Steinschneider, S. and Brown, C., 2013. A semiparametric multivariate, multisite weather generator with low-frequency variability for use in climate risk assessments. *Water Resources Research*, 49 (11), 7205–7220. doi:10.1002/wrcr.20528.
- Steinschneider, S., Wi, S., and Brown, C., 2015b. The integrated effects of climate and hydrologic uncertainty on future flood risk assessments. *Hydrological Processes*, 29 (12), 2823–2839. doi:10.1002/hyp.10409.
- Stephenson, D.B., et al., 2012. Statistical problems in the probabilistic prediction of climate change. *Environmetrics*, 23, 364–372. doi:10.1002/env.2153
- Tebaldi, C. and Knutti, R., 2007. The use of the multi-model ensemble in probabilistic climate projections. *Philosophical Transactions of the Royal Society A: Mathematical, Physical and Engineering Sciences*, 365 (1857), 2053–2075. doi:10.1098/rsta.2007.2076.
- Témez, J.R., 1977. *Modelo matemático de transformación "precipitación-aportación"*. Madrid: Asociación de Investigación Industrial Eléctrica (ANISEL).
- Tsanis, I.K., et al., 2011. Severe climate-induced water shortage and extremes in Crete. *Climatic Change*, 106 (4), 667–677. doi:10.1007/s10584-011-0048-2.
- UNESCO, 2018. *Climate Risk Informed Decision Analysis (CRIDA)*. Paris: Unesco.
- Visser, P.M., et al., 2016. How rising CO₂ and global warming may stimulate harmful cyanobacterial blooms. *Harmful Algae*, 54, 145–159. doi:10.1016/j.hal.2015.12.006

Appendix

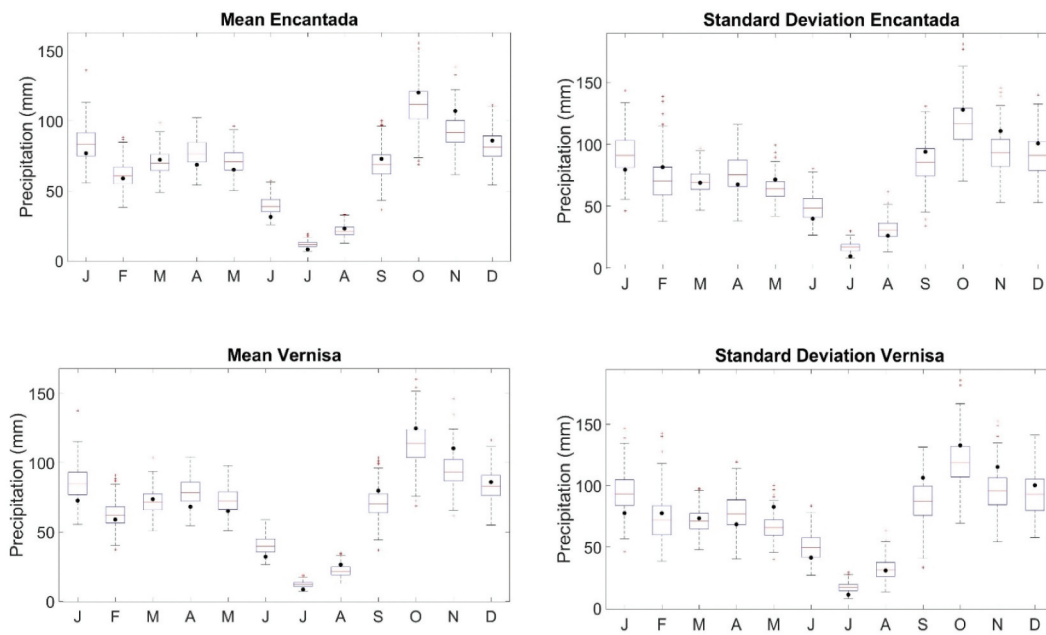


Figure A1. Mean and standard deviation of the 434 synthetic simulations over the 65-year monthly time series of precipitation in the Encantada (a, b) and Vernisa (c, d) sub-basins.

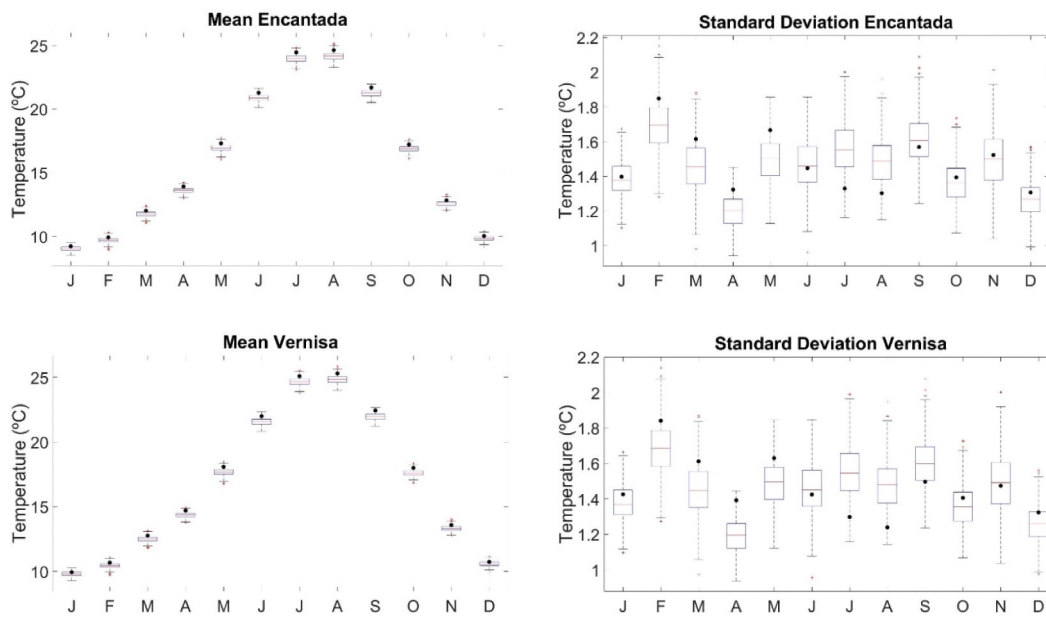


Figure A2. Mean and standard deviation of the 434 synthetic simulations over the 65-year monthly precipitation time series in the Encantada (a, b) and Vernisa (c, d) sub-basins.

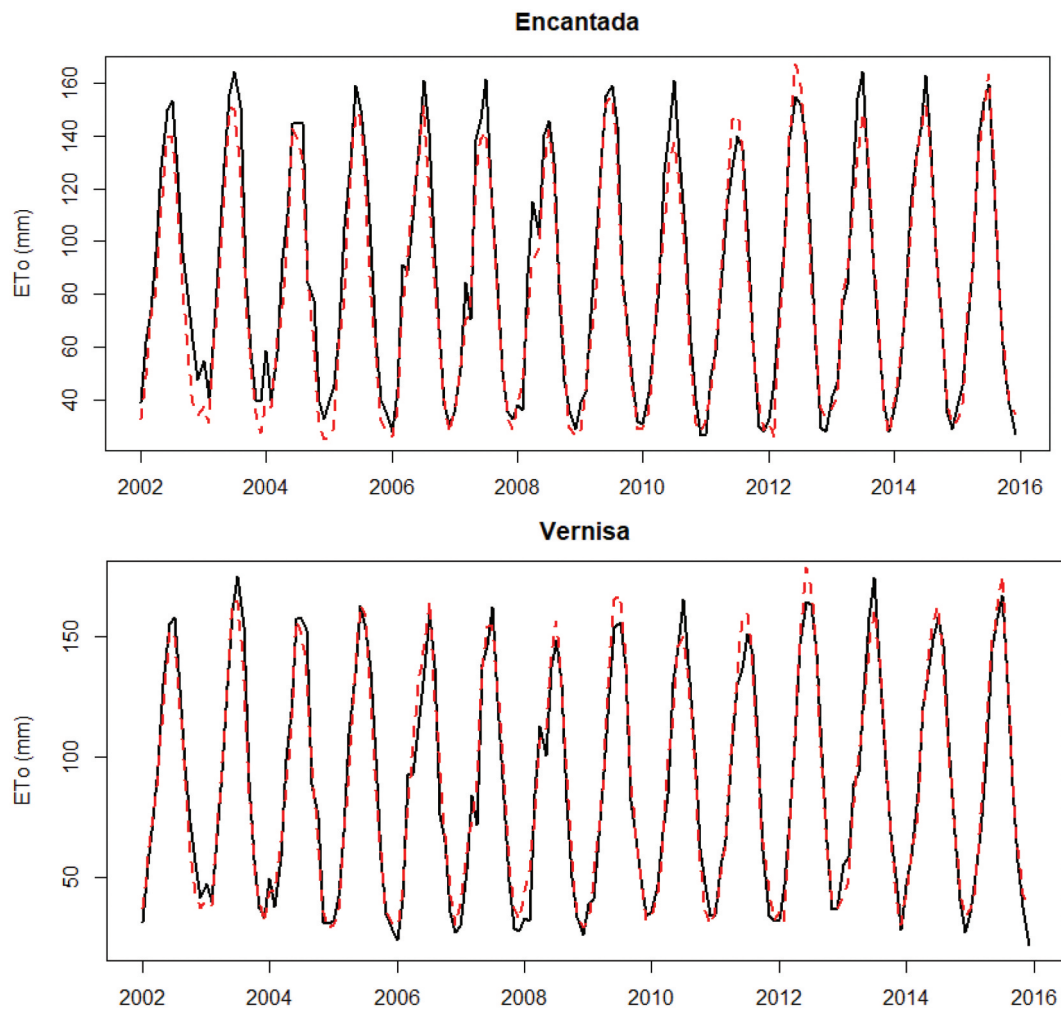


Figure A3. Historical (black) and estimated (dashed red) reference evapotranspiration (ETo) monthly time series in the Encantada and Vernisa sub-basins.

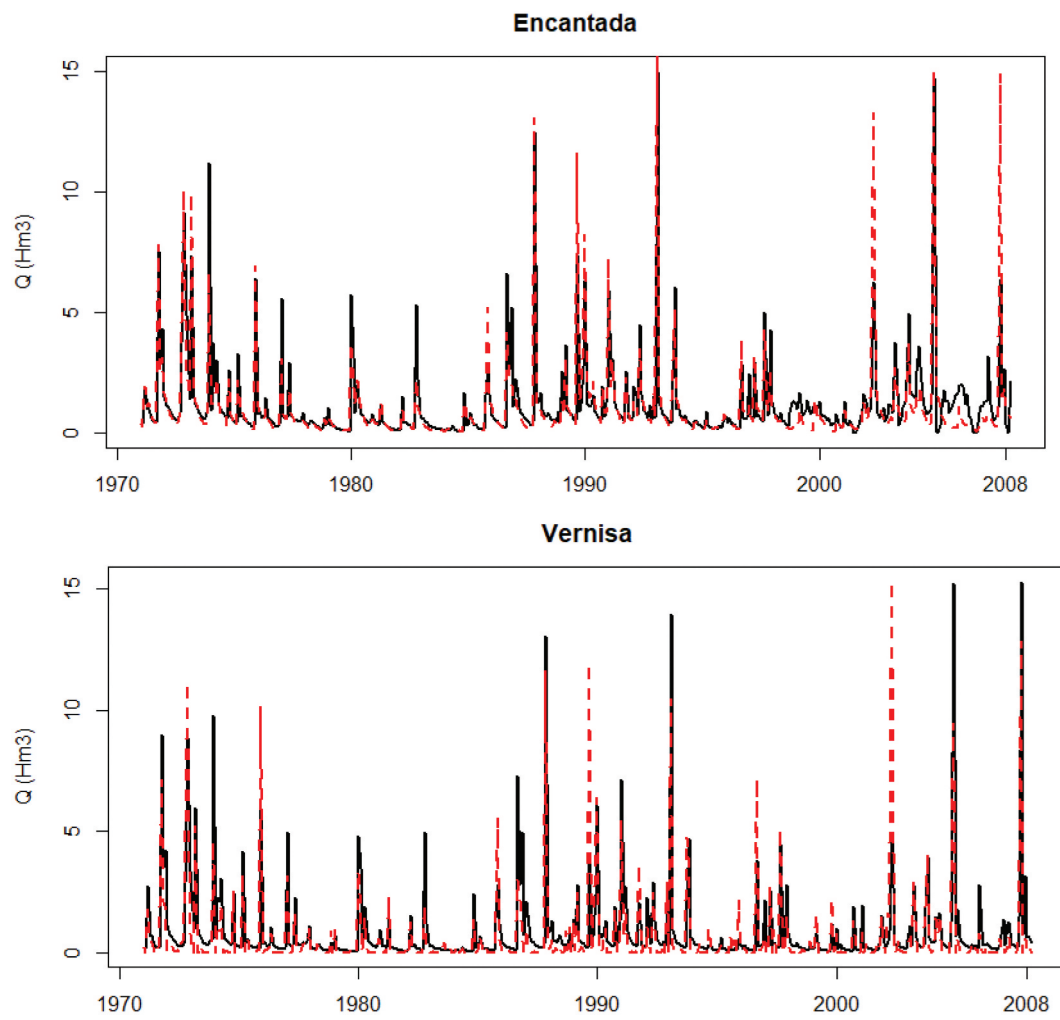


Figure A4. Historical (black) and estimated (dashed red) hydrographs in the Encantada and Vernisa sub-basins.

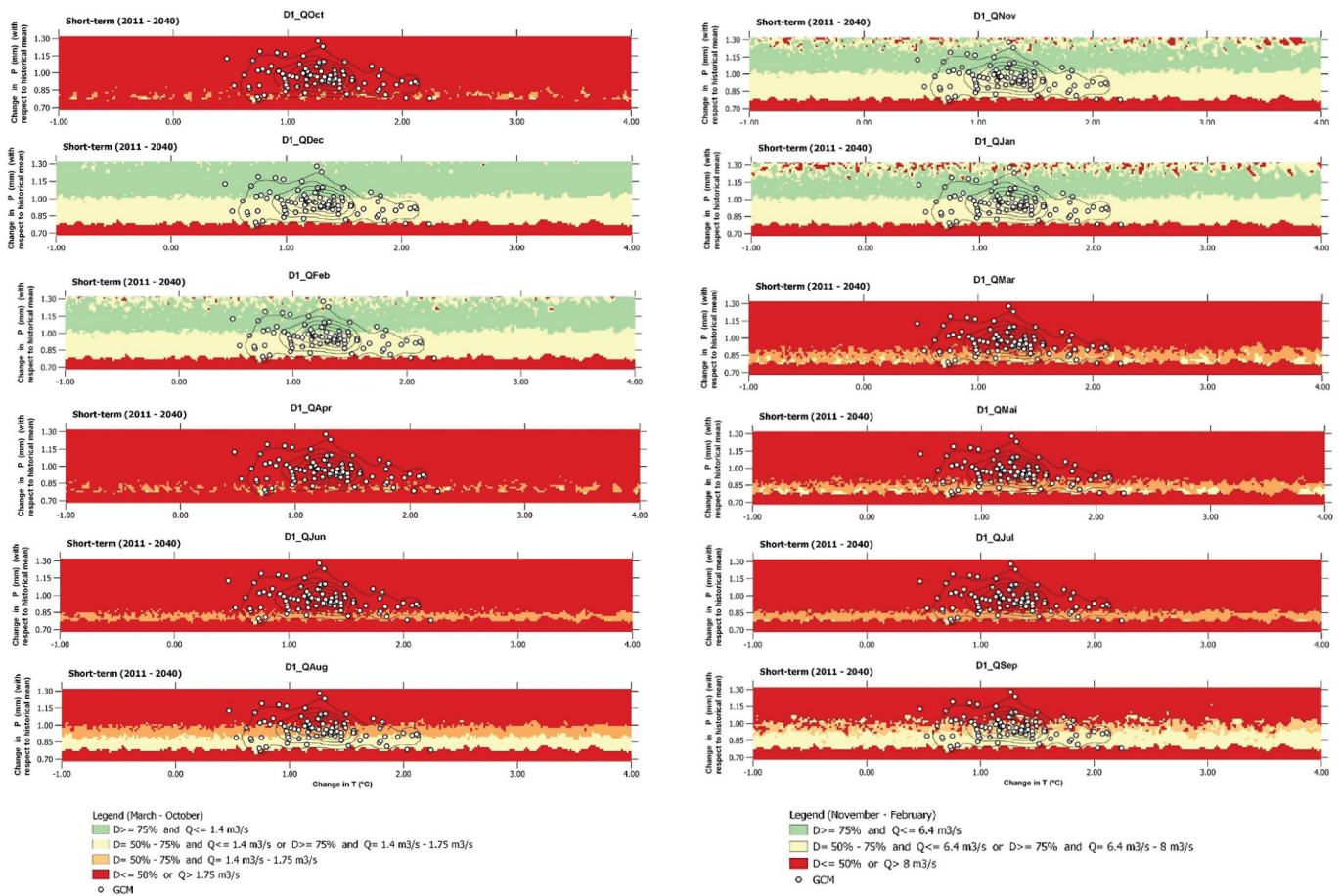


Figure A5. Overlapping maps of mutually acceptable performance (trade-off space) for the two indicators (agricultural demand supply and environmental maximum flow) for agricultural demand 1 (D1) and the mean monthly flow (Q) in the study river reach across a range of climatic conditions. The white dots represent an ensemble of Global Climate Model (GCM) projections from Coupled Model Intercomparison Project Phase 6 (CMIP6) in the short term (2011–2040).

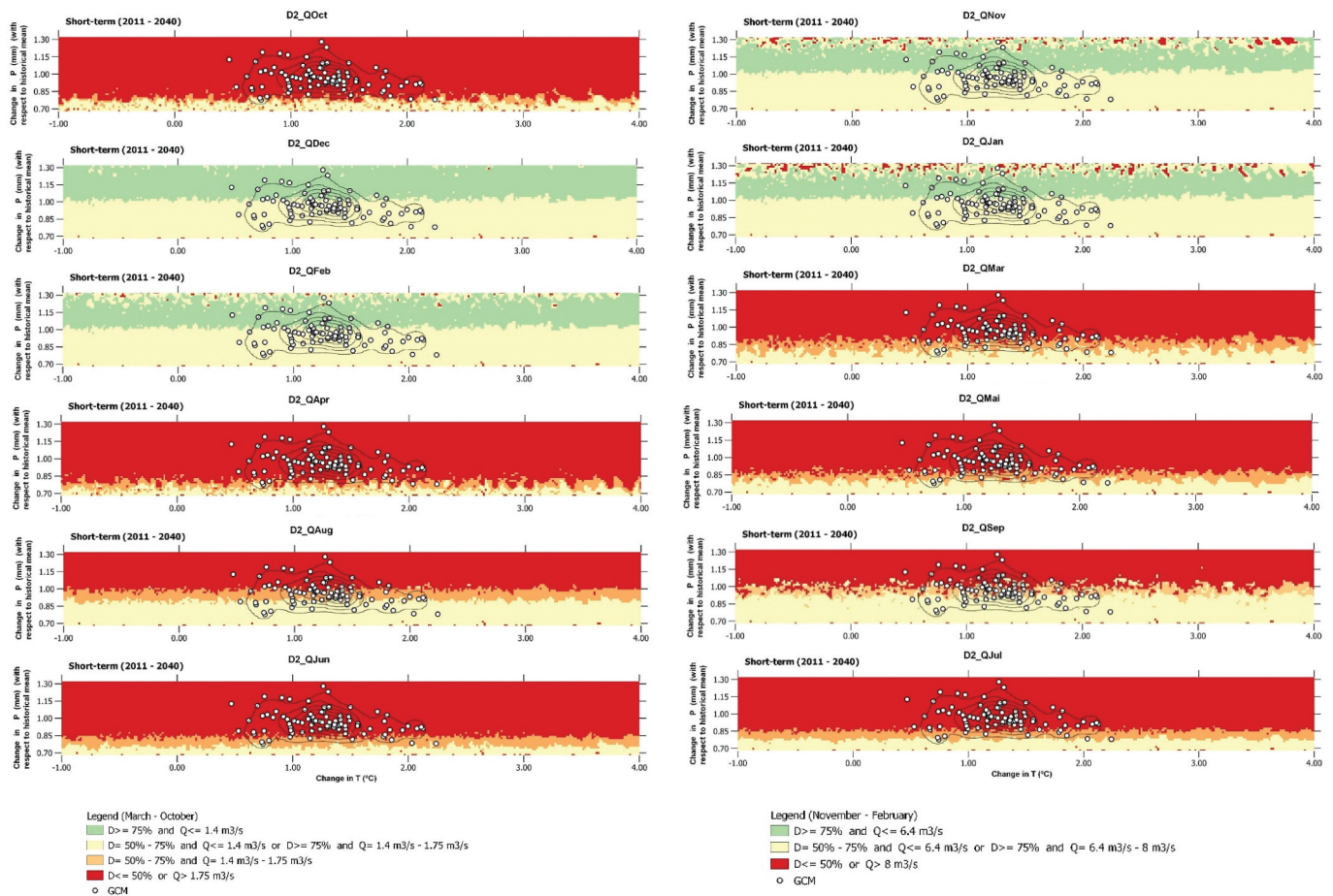


Figure A6. Overlapping maps of mutually acceptable performance (trade-off space) for the two indicators (agricultural demand supply and environmental maximum flow) for agricultural demand 2 (D2) and the mean monthly flow (Q) in the study river reach across a range of climatic conditions. The white dots represent an ensemble of GCM projections from CMIP6 in the short term (2011–2040).

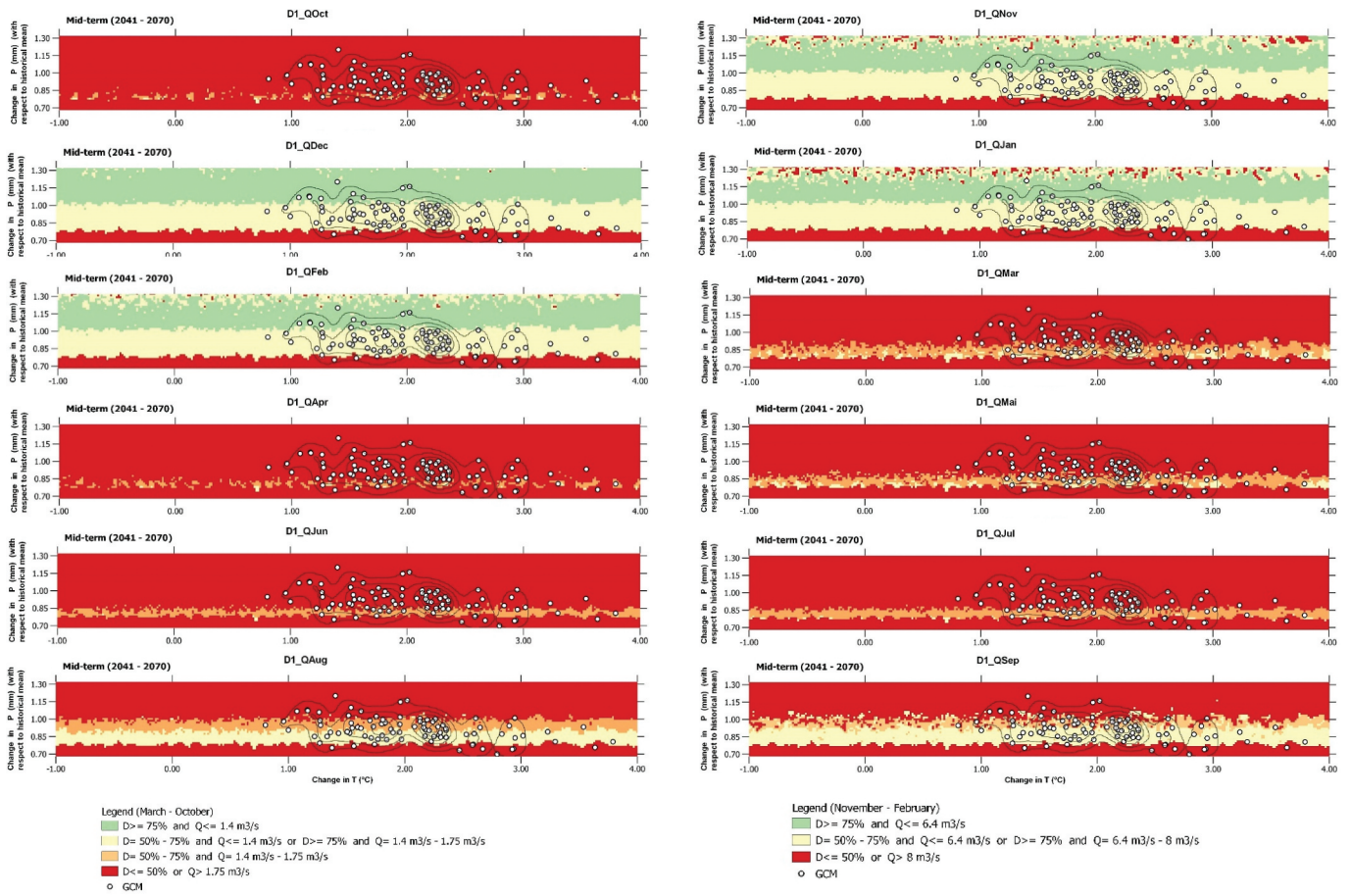


Figure A7. Overlapping maps of mutually acceptable performance (trade-off space) for the two indicators (agricultural demand supply and environmental maximum flow) for agricultural demand 1 (D1) and the mean monthly flow (Q) in the study river reach across a range of climatic conditions. The white dots represent an ensemble of GCM projections from CMIP6 in the mid term (2041–2070).

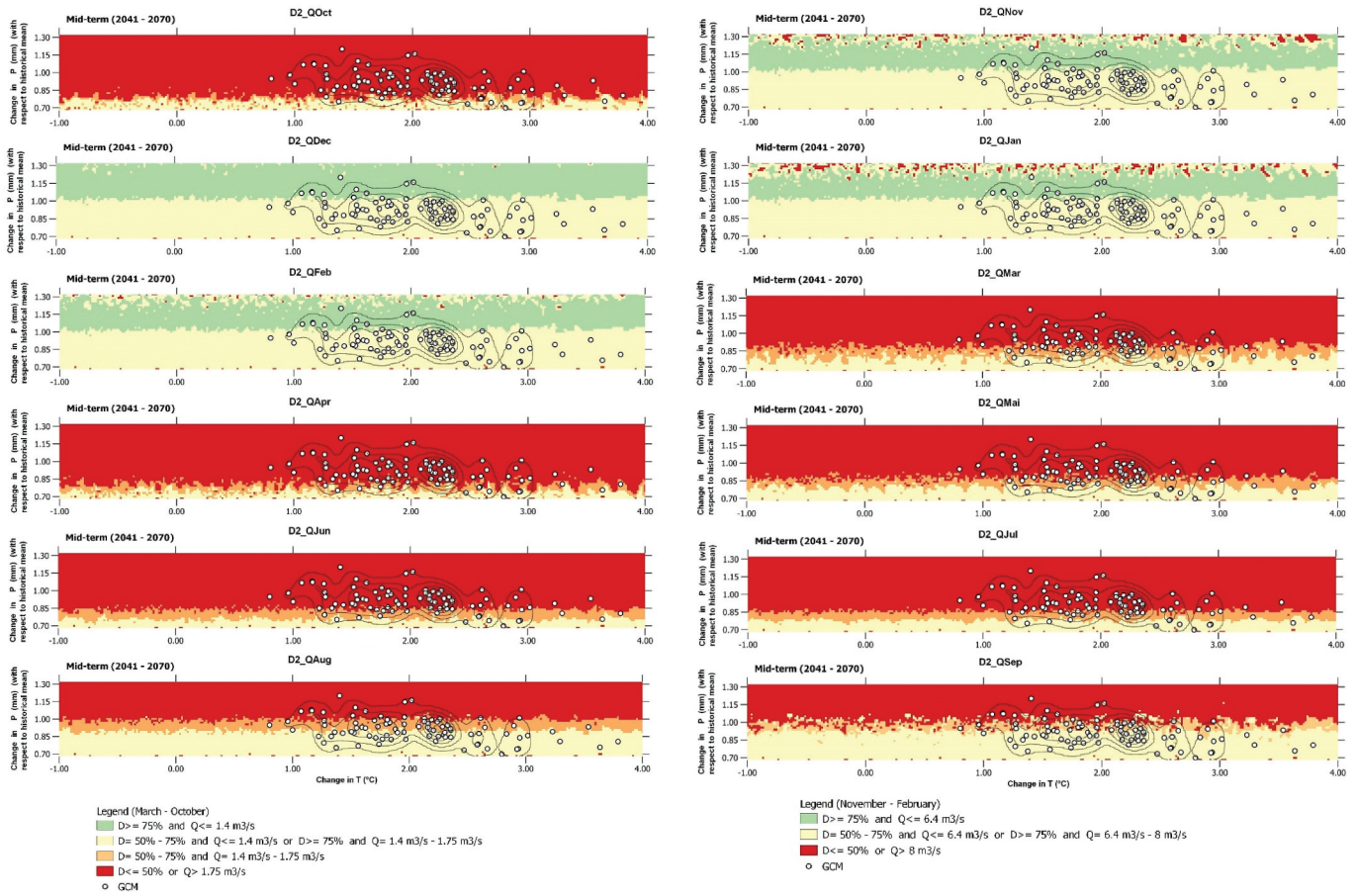


Figure A8. Overlapping maps of mutually acceptable performance (trade-off space) for the two indicators (agricultural demand supply and environmental maximum flow) for agricultural demand 2 (D2) and the mean monthly flow (Q) in the study river reach across a range of climatic conditions. The white dots represent an ensemble of GCM projections from CMIP6 in the mid term (2041–2070).

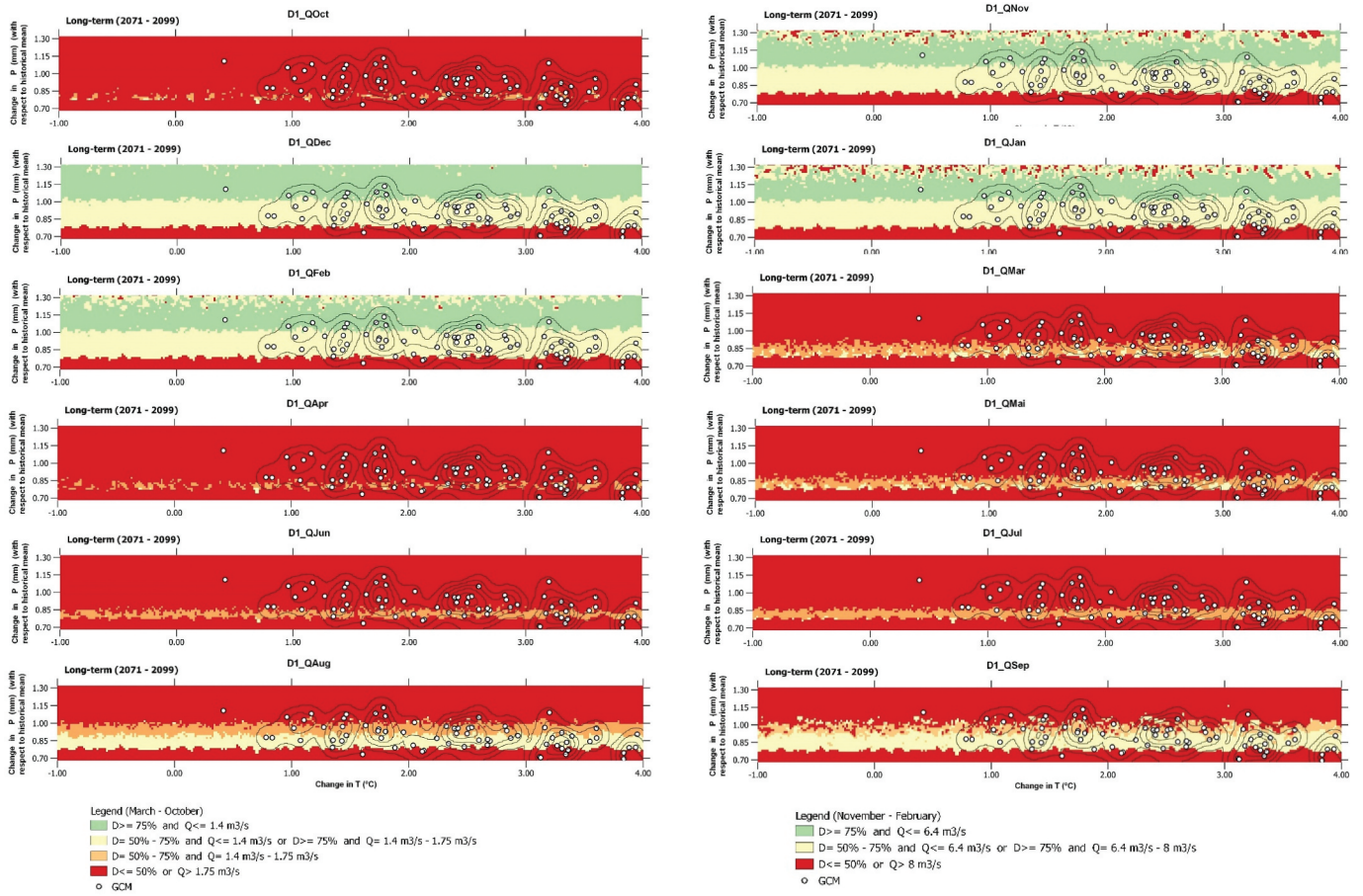


Figure A9. Overlapping maps of mutually acceptable performance (trade-off space) for the two indicators (agricultural demand supply and environmental maximum flow) for agricultural demand 1 (D1) and the mean monthly flow (Q) in the study river reach across a range of climatic conditions. The white dots represent an ensemble of GCM projections from CMIP6 in the long term (2071–2090).

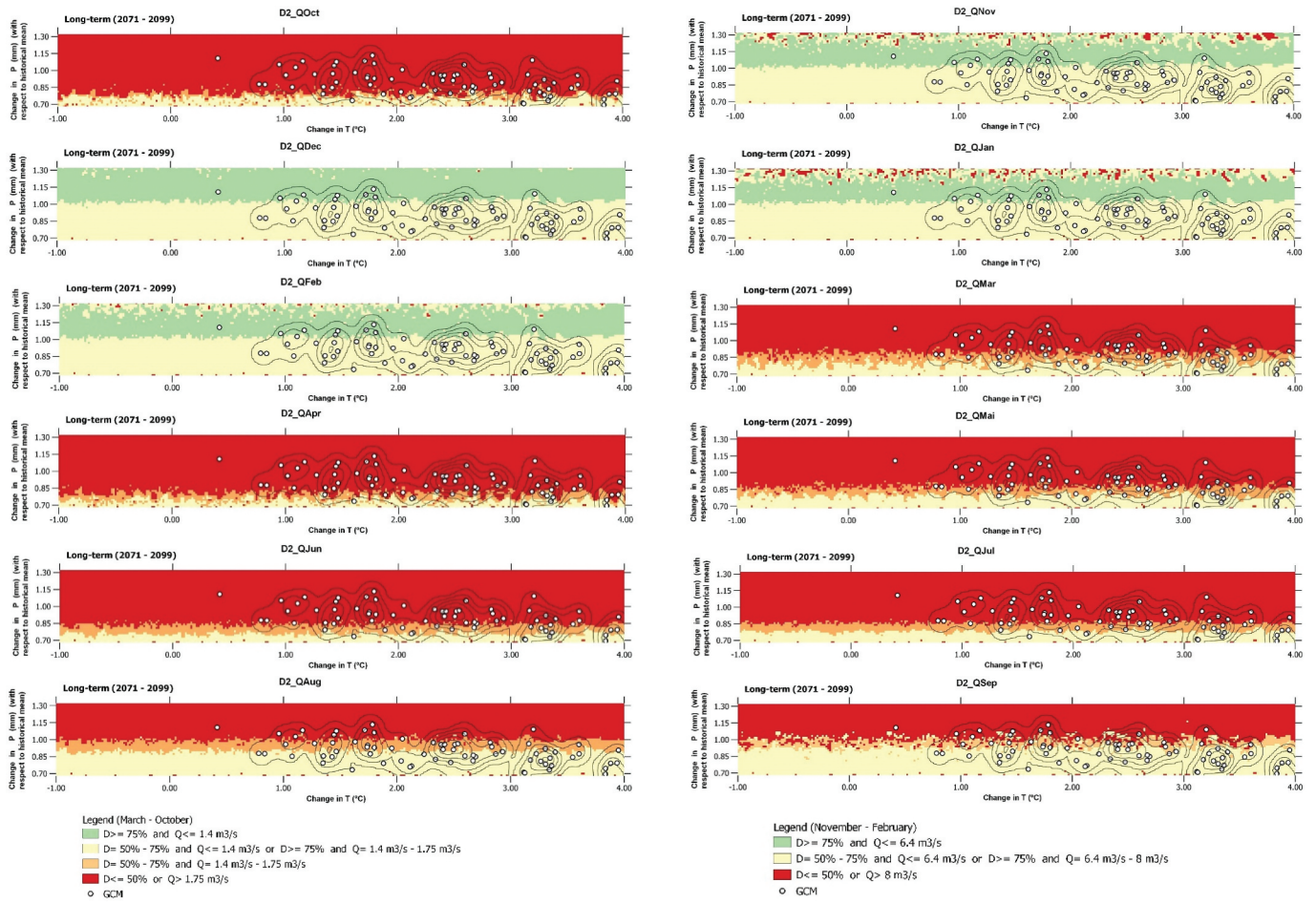


Figure A10. Overlapping maps of mutually acceptable performance (trade-off space) for the two indicators (agricultural demand supply and environmental maximum flow) for agricultural demand 2 (D2) and the mean monthly flow (Q) in the study river reach across a range of climatic conditions. The white dots represent an ensemble of GCM projections from CMIP6 in the long term (2071–2090).